62-1-3
XEROX

TECHNICAL NOTE

D-1102

CONSISTENT P1 ANALYSIS OF AQUEOUS URANIUM-235

CRITICAL ASSEMBLIES

By Daniel Fieno

Lewis Research Center
Cleveland, Ohio

NATIONAL AERONAUTICS AND SPACE ADMINISTRATION

WASHINGTON   November 1961

NATIONAL AERONAUTICS AND SPACE ADMINISTRATION

TECHNICAL NOTE D-1102

CONSISTENT P1 ANALYSIS OF AQUEOUS URANIUM-235

CRITICAL ASSEMBLIES

By Daniel Fieno

SUMMARY

The lethargy-dependent equations of the consistent P1 approximation to the Boltzmann transport equation for slowing down neutrons have been used as the basis of an IBM 704 computer program. Some of the effects included are (1) linearly anisotropic center of mass elastic scattering, (2) heavy element inelastic scattering based on the evaporation model of the nucleus, and (3) optional variation of the buckling with lethargy. The microscopic cross-section data developed for this program covered 473 lethargy points from lethargy $u = 0$ (10 Mev) to $u = 19.8$ (0.025 ev).

The value of the fission neutron age in water calculated here is 26.5 square centimeters; this value is to be compared with the recent experimental value given as 27.86 square centimeters. The Fourier transform of the slowing-down kernel for water to indium resonance energy calculated here compared well with the Fourier transform of the kernel for water as measured by Hill, Roberts, and Fitch.

This method of calculation has been applied to uranyl fluoride - water solution critical assemblies. Theoretical results established for both unreflected and fully reflected critical assemblies have been compared with available experimental data. The theoretical buckling curve derived as a function of the hydrogen to uranium-235 atom concentration for an energy-independent extrapolation distance was successful in predicting the critical heights of various unreflected cylindrical assemblies. The critical dimensions of fully water-reflected cylindrical assemblies were reasonably well predicted using the theoretical buckling curve and reflector savings for equivalent spherical assemblies.

INTRODUCTION

The NASA Lewis Research Center has for some time operated a Zero Power Reactor. This reactor consists of uranyl fluoride salt (UO_2F_2)

dissolved in water and contained in a cylindrical aluminum tank. The parameters of the system are the diameter of the cylindrical tank, use of a side reflector, and concentration of uranyl fluoride salt in water. Criticality is achieved by varying the height of the solution in the tank. No control rods are inserted into the solution while the reactor is critical. Thus, good experimental conditions exist for obtaining criticality data and performing reactivity measurements by measuring changes in the solution height due to insertions in the reactor. Description of this reactor and its various characteristics are found in the final hazards report (ref. 1) prepared for the Atomic Energy Commission.

The criticality data obtained from the NASA Zero Power Reactor as well as that obtained from extensive experimental studies performed at the Oak Ridge National Laboratory (refs. 2, 3, and 4) can be analyzed by various theoretical models. Callihan (ref. 5) describes the use of Fermi age-diffusion and Goertzel-Selengut analytical models as well as a method due to Greuling for predicting critical reactor diameters of various Oak Ridge experiments. A more recent study of the Oak Ridge experimental data by Gwin and others (ref. 6) makes use of the empirical kernel method, which is based on the measured slowing-down distribution in water rather than on any theoretical model of the neutron slowing-down process. In addition, the use of the Los Alamos DSN transport code for obtaining minimum critical dimensions for water solution is described by Mills (ref. 7).

The objective of the present study is to provide a theoretical model based on the numerical solution of the lethargy-dependent consistent P1 approximation to the Boltzmann transport equation for slowing down neutrons. This model is coded for the IBM 704 electronic computer and employs microscopic nuclear data (refs. 8, 9, and 10). This theoretical model is tested by comparison with the experimental age and Fourier transform of the slowing-down kernel of fission neutrons in water. This model is further employed in estimating the absolute reactivity of unreflected UO_2F_2-water systems and is used as a basis for evaluating consistent three-group parameters for the interpretation of water-reflected UO_2F_2-water systems.

The next section gives the derivation of the general lethargy-dependent consistent P1 equations used as the basis for an IBM 704 code. Next follows a section giving the analytical results based on this model and comparison with experimental data obtained with the NASA Zero Power Reactor as well as data obtained at Oak Ridge.

THEORY

Slab Geometry Spherical Harmonics Form of Transport Equation

Let $n(\vec{r},\vec{v})d\vec{r}\,d\vec{v}$ be the probable number of neutrons in the space volume element $d\vec{r}$ about position $\vec{r}$ and in the velocity element $d\vec{v}$

about velocity $\vec{v}$ per unit time. Then, the Boltzmann transport equation for slowing down neutrons at steady-state, which equates the losses per unit time of neutrons, due to transport out of and collision removal from the phase volume element $d\vec{r}\, d\vec{v}$, to the gain per unit time of neutrons, due to elastic and inelastic in-scattering and fissioning of the fissile nuclei in the phase volume element $d\vec{r}\, d\vec{v}$, has the form

$$\vec{\Omega} \cdot \nabla\varphi(\vec{r},\vec{v}) + \Sigma_t(v)\varphi(\vec{r},\vec{v}) = \int d\vec{v}'\Sigma_{es}(v')\varphi(\vec{r},\vec{v}')P(\vec{v}' \to \vec{v})$$

$$+ \int d\vec{v}'\Sigma_{in}(v')\varphi(\vec{r},\vec{v}')H(\vec{v}' \to \vec{v}) + S(\vec{r},\vec{v}) \qquad (1)$$

where the neutron flux is defined as $\varphi(\vec{r},\vec{v}) = vn(\vec{r},\vec{v})$ with v being the neutron speed; $S(\vec{r},\vec{v})$ is the source of neutrons due to fission; $\Sigma_t(v)$, $\Sigma_{es}(v)$, $\Sigma_{in}(v)$ are the macroscopic total, elastic scattering, and inelastic scattering cross sections, respectively, at speed v; $\vec{\Omega}$ is a unit vector along the direction of motion of the neutron; $P(\vec{v}' \to \vec{v})$ is the probability that a neutron in the phase volume element $d\vec{r}\, d\vec{v}'$ will, after an elastic scattering collision, be in the phase volume $d\vec{r}\, d\vec{v}$. Similarly, $H(\vec{v}' \to \vec{v})$ is the probability that a neutron in the phase volume element $d\vec{r}\, d\vec{v}'$ will, after an inelastic scattering collision, be in the phase volume $d\vec{r}\, d\vec{v}$.

Now transform equation (1) from $(\vec{r},\vec{v})$ space to $(\vec{r},v,\vec{\Omega})$ space and finally from $(\vec{r},v,\vec{\Omega})$ space to $(\vec{r},u,\vec{\Omega})$ space where u is the neutron lethargy defined by the relation $u = \ln(E_0/E)$ with E_0 usually taken as 10^7 ev. The result of these transformations and writing an explicit form for the fission source is

$$\vec{\Omega} \cdot \nabla\varphi(\vec{r},u,\vec{\Omega}) + \Sigma_t(u)\varphi(\vec{r},u,\vec{\Omega}) = \int du'\Sigma_{es}(u') \int d\Omega'\varphi(\vec{r},u';\vec{\Omega}')P(u-u';\mu_L)$$

$$+ \int du'\Sigma_{in}(u') \frac{H(u' \to u)}{4\pi} \int d\Omega'\varphi(\vec{r},u;\vec{\Omega}')$$

$$+ \frac{f(u)}{4\pi K_{eff}} \int du'\nu(u')\Sigma_f(u') \int d\Omega'\varphi(\vec{r},u;\vec{\Omega}') \qquad (2)$$

where $\nu(u)$ is the number of neutrons released per fission occurring at lethargy u, $\Sigma_f(u)$ is the macroscopic fission cross section, $f(u)$ is the fraction of the fission neutrons born in the lethargy element du about u (the integral of $f(u)$ over all lethargies is normalized to unity), K_{eff} is the static criticality factor, and $d\Omega$ is the element of solid angle about the direction $\vec{\Omega}$. The inelastic scattering kernel is assumed to depend only on the initial lethargy u' and the final lethargy u of an inelastically scattered neutron and to be isotropic in the laboratory coordinate system. The elastic scattering kernel is assumed to

4

depend only on the difference between the final and initial lethargies and on the cosine of the angle μ_L between the initial and final directions of motion of a neutron undergoing an elastic scattering collision. Davison (ch. II, ref. 11) gives additional details concerning equation (2).

If the neutron distribution varies only along the Z-direction and is azimuthally symmetric about that axis, if equation (2) is integrated over the azimuthal angle, and if the flux φ $(= \varphi(Z, u, \mu)$ (the quantity μ is the cosine of the angle between the Z-direction and the direction of neutron motion $\vec{\Omega}$) and the elastic scattering kernel are expanded into a series of Legendre polynomials, that is,

$$\varphi(Z, u, \mu) = \sum_{l=0}^{\infty} \frac{2l + 1}{2} \varphi_l(Z, u) P_l(\mu) \qquad (3a)$$

$$P(u-u; \mu_L) = \sum_{l=0}^{\infty} \frac{2l + 1}{2} P_l(u-u') P_l(\mu_L) \qquad (3b)$$

and these expansions are substituted into the equation for $\varphi(Z, u, \mu)$, which is then multiplied by a Legendre polynomial $P_K(\mu)$ and integrated over all μ, then the result will be the infinite sequence of integro-differential equations given as

$$\frac{\partial}{\partial Z} \left[\frac{l}{2l + 1} \varphi_{l-1}(Z, u) + \frac{l + 1}{2l + 1} \varphi_{l+1}(Z, u) \right] + \Sigma_t(u) \varphi_l(Z, u)$$

$$= \int du' \Sigma_{es}(u') \varphi_l(Z, u') P_l(u-u') + \delta_{0,l} \int du' \Sigma_{in}(u') \varphi_0(Z, u') H(u' \to u)$$

$$+ \delta_{0,l} \frac{f(u)}{K_{eff}} \int_0^{\infty} du' \nu(u') \Sigma_f(u') \varphi_0(Z, u'); \quad (l = 0, 1, 2, \ldots, \infty) \quad (4)$$

where $\delta_{0,l}$ is the Kronecker delta defined here by the properties

$$\delta_{0,l} = 1, \quad l = 0$$

$$= 0, \quad l \neq 0 \qquad (5)$$

Equation (4) represents the spherical harmonics form of the transport equation in slab geometry.

Slab Geometry Spherical Harmonics Form of Angular Slowing-

Down Density Due to Elastic Scattering

Another important characteristic of slowing down neutrons is the slowing-down density $Q(\vec{r}, u, \vec{\Omega})$. The slowing-down density due to elastic scattering $Q(\vec{r}, u, \vec{\Omega})$ is defined as the number of neutrons which pass the lethargy mark u per unit time per unit phase volume $(d\vec{r}\, d\Omega)$. This quantity is easily derivable as

$$Q(\vec{r}, u, \vec{\Omega}) = \int_0^u du' \int_u^\infty du'' \int_{\vec{\Omega}'} d\Omega' \Sigma_{es}(u') \varphi(\vec{r}, u; \vec{\Omega}') P(u'' - u; \mu_L) \quad (6)$$

If the slowing-down density varies only along the Z-direction and is azimuthally symmetric about that axis, if equation (6) is integrated over the azimuth angle φ, if the expressions for $\varphi(Z, u, \mu)$ and $P(u-u; \mu_L)$, given by equations (3a) and (3b), respectively, are substituted into (6) and then integrated over $d\Omega'$, and if the resulting equation is multiplied by a Legendre polynomial $P_K(\mu)$ and integrated over all μ, then the result will be the moments $Q_l(Z, u)$ of the slowing-down density $Q(Z, u, \vec{\Omega})$; that is,

$$Q_l(Z, u) = \int d\Omega Q(Z, u, \vec{\Omega}) P_l(\mu) = \int_0^u du' \int_u^\infty du'' \Sigma_{es}(u') \varphi_l(Z, u') P_l(u'' - u')$$

$$(l = 0, 1, 2, \ldots, \infty) \quad (7)$$

Equation (7) represents the spherical harmonics form of the slowing-down density in slab geometry.

Lethargy-Dependent Consistent P1 Equations in Slab Geometry

To obtain the P1 equations from equation (4) the assumption is now made that $\varphi_l(Z, u) \equiv 0$ for $l \geq 2$, which implies for equation (7) that $Q_l(Z, u) \equiv 0$ for $l \geq 2$ also. The lethargy-dependent consistent P1 equations can now be obtained by assuming the following spatial and lethargy dependence for $\varphi_0(Z, u)$ and $\varphi_1(Z, u)$:

$$\varphi_0(Z, u) = \varphi(u) G[B_m(u) Z] \quad (8a)$$

$$\varphi_1(Z, u) = J(u) F[B_m(u) Z] \quad (8b)$$

6

In addition, the material buckling $B_m(u)$ is assumed to be a slowly varying function of lethargy. Therefore, the integral terms arising in equation (4) can be evaluated by taking

$$\varphi_0(Z,u') \doteq \varphi(u')G\left[B_m(u)Z\right] \tag{8c}$$

$$\varphi_1(Z,u') \doteq J(u')F\left[B_m(u)Z\right] \tag{8d}$$

The lethargy and space variation for the $l = 0,1$ terms of equation (7) follows from equations (8a) and (8b) and is

$$Q_0(Z,u) = Q(u)G\left[B_m(u)Z\right] \tag{8e}$$

$$Q_1(Z,u) = P(u)F\left[B_m(u)Z\right] \tag{8f}$$

where G and F are spatial functions and $B_m(u)$ is defined as the lethargy-dependent material buckling. In addition, the spatial functions G and F must satisfy the conditions

$$\frac{\partial}{\partial Z}\left\{G\left[B_m(u)Z\right]\right\} = -B_m(u)F\left[B_m(u)Z\right] \tag{9a}$$

$$\frac{\partial}{\partial Z}\left\{F\left[B_m(u)Z\right]\right\} = B_m(u)G\left[B_m(u)Z\right] \tag{9b}$$

With the assumptions implied by equations (8a) to (8d) and (9a) and (9b), the spatial dependence can be divided out, and the lethargy-dependent consistent P1 equations obtained from equation (4) are

$$B_m(u)J(u) + \Sigma_t(u)\varphi(u) = \int du'\Sigma_{es}(u')\varphi(u')P_0(u-u')$$

$$+ \int du'\Sigma_{in}(u')\varphi(u')H(u' \rightarrow u)$$

$$+ \frac{f(u)}{K_{eff}}\int_0^\infty du'\nu(u')\Sigma_f(u')\varphi(u') \tag{10a}$$

$$-\frac{1}{3}B_m(u)\varphi(u) + \Sigma_t(u)J(u) = \int du'\Sigma_{es}(u')J(u')P_1(u-u') \tag{10b}$$

together with

$$Q(u) = \int_0^u du' \int_u^\infty du''\Sigma_{es}(u')\varphi(u')P_0(u'' - u') \tag{11a}$$

$$P(u) = \int_0^u du' \int_u^\infty du'' \Sigma_{es}(u')J(u')P_1(u'' - u') \qquad (11b)$$

In reference 12 Simon discusses some analytical solutions of the lethargy-dependent consistent P1 equations for hydrogen. To obtain the analytical results, special cross-section variations were assumed for hydrogen.

Elastic Scattering Kernel for Linearly Anisotropic

Center of Mass Elastic Scattering

Since most light elements exhibit anisotropic elastic scattering in the center of mass coordinate system for high-energy neutrons, it is important to include this effect if accurate values of the neutron age are to be computed. Therefore, by following Marshak (ref. 13) it is easy to show that for linearly anisotropic scattering in the center of mass coordinate system the elastic scattering kernel $P(u-u;\mu_L)$ is given by

$$P(u-u;\mu_L)du \; d\mu_L \; d\varphi_L$$

$$= \frac{(A + 1)^2}{8\pi A} e^{-(u-u')}\left\{1 + 3f_1(u')\left[\frac{(A + 1)^2}{2A} e^{-(u-u')}\right.\right.$$

$$\left.\left. - \frac{A^2 + 1}{2A}\right]\right\}\delta\left\{\mu_L(u-u') - \left[\frac{A + 1}{2} e^{-\frac{1}{2}(u-u')} - \frac{A - 1}{2} e^{\frac{1}{2}(u-u')}\right]\right\}$$

$$\times du \; d\mu_L \; d\varphi_L \qquad (12)$$

where $f_1(u)$ is the average cosine of the angle between the initial and final direction of motion in the center of mass coordinate system of the elastically scattered neutron of initial lethargy u, A is the ratio of the mass of the scattering nucleus to that of the neutron, δ is the Dirac delta function, and φ_L is an appropriate azimuthal angle in the laboratory coordinate system. The moments $P_l(u-u')$ of the expansion of $P(u-u;\mu_L)$ into a series of Legendre polynomials, as in equation (3b), are given by the orthogonality property of these polynomials as

$$P_l(u-u') = \int d\Omega_L P_l(\mu_L)P(u-u;\mu_L) \qquad (13)$$

Substituting equation (12) into equation (13) and performing the indicated integrations for $l = 0, 1$ will give

$$P_0(u-u') = \frac{(A+1)^2}{4A} e^{-(u-u')} \left\{ 1 + 3f_1(u') \left[\frac{(A+1)^2}{2A} e^{-(u-u')} \right. \right.$$

$$\left. \left. - \frac{A^2+1}{2A} \right] \right\}, \quad -1 \leq \mu_L(u-u') \leq 1$$

$$= 0, \text{ otherwise} \tag{14a}$$

$$P_1(u-u') = \mu_L(u-u')P_0(u-u'), \quad -1 \leq \mu_L(u-u') \leq 1$$

$$= 0, \text{ otherwise} \tag{14b}$$

If $t = u-u'$, equations (14a) and (14b) can be rewritten into the following useful forms:

$$P_0(t) = \frac{(A+1)^2}{4A} e^{-t} + f_1(u') \left[\frac{3(A+1)^4}{8A^2} e^{-2t} - \frac{3(A^2+1)(A+1)^2}{8A^2} e^{-t} \right] \tag{15a}$$

$$P_1(t) = \frac{(A+1)^3}{8A} e^{-\frac{3}{2}t} - \frac{(A-1)(A+1)^2}{8A} e^{-\frac{1}{2}t}$$

$$+ f_1(u') \left[\frac{3(A+1)^5}{16A^2} e^{-\frac{5}{2}t} - \frac{3(A+1)^3}{8} e^{-\frac{3}{2}t} \right.$$

$$\left. + \frac{3(A-1)(A^2+1)(A+1)^2}{16A^2} e^{-\frac{1}{2}t} \right] \tag{15b}$$

Equations (15a) and (15b) reduce to their isotropic center of mass elastic scattering values if $f_1(u') \cong 0$.

Differential Form of Consistent P1 Equations

Although equations (10a) and (10b) are the lethargy-dependent consistent P1 equations, a differential form of these equations would be more suitable for computation. To obtain these differential equations differentiate equations (11a) and (11b) with respect to lethargy u:

$$\frac{dQ(u)}{du} = - \int_0^u du' \Sigma_{es}(u')\varphi(u')P_0(u-u') + \Sigma_{es}(u)\varphi(u) \int_u^\infty du'' P_0(u''-u)$$

$$= - \int_0^u du' \Sigma_{es}(u')\varphi(u')P_0(u-u') + \Sigma_{es}(u)\varphi(u) \tag{16a}$$

$$\frac{dP(u)}{du} = -\int_0^u du' \Sigma_{es}(u') J(u') P_1(u-u') + \Sigma_{es}(u) J(u) \int_u^\infty du'' P_1(u'' - u)$$

$$= -\int du' \Sigma_{es}(u') J(u') P_1(u-u') + \mu_0(u) \Sigma_{es}(u) J(u) \qquad (16b)$$

The integral $\int_u^\infty du'' P_0(u'' - u)$ is evaluated using equation (15a) and is equal to unity. The integral $\int_u^\infty du'' P_1(u'' - u)$ is evaluated using (15b) and is equal to $\mu_0(u)$ - the average cosine of the angle between the initial and final direction of motion, as measured in the laboratory coordinate system, of the elastically scattered neutrons. The first integral on the right side of equation (10a) can be evaluated using equation (16a), and the integral term on the right side of equation (10b) can be evaluated using equation (16b). Equations (10a) and (10b) now become

$$B_m(u) J(u) + [\Sigma_a(u) + \Sigma_{in}(u)] \varphi(u) + \frac{dQ(u)}{du}$$

$$= \frac{f(u)}{K_{eff}} \int_0^\infty du' \nu(u') \Sigma_f(u') \varphi(u') + \int du' \Sigma_{in}(u') \varphi(u') H(u' \to u) \qquad (17a)$$

$$-\frac{1}{3} B_m(u) \varphi(u) + [\Sigma_t(u) - \mu_0(u) \Sigma_{es}(u)] J(u) + \frac{dP(u)}{du} = 0 \qquad (17b)$$

where $\Sigma_a(u)$ is the macroscopic absorption cross section. Equations (17a) and (17b) represent the basic lethargy-dependent equations of the consistent P1 approximation to the Boltzmann transport equation for slowing-down neutrons.

Two more equations are needed to complete the P1 description of the slowing-down process as given by equations (17a) and (17b). These are coupling equations between $\varphi(u)$ and $Q(u)$, and $J(u)$ and $P(u)$, which can be obtained by writing approximate forms for equations (11) and (16). These additional equations are obtained in the following manner. Assume that the functions $\Sigma_{es}(u') \varphi(u')$ and $\Sigma_{es}(u') J(u')$ are slowly varying functions and that they can be approximated by the first two terms of a Taylor's series expansion about lethargy u. That is,

$$\Sigma_{es}(u') \varphi(u') \doteq \Sigma_{es}(u) \varphi(u) + (u' - u) \frac{d}{du} [\Sigma_{es}(u) \varphi(u)] \qquad (18a)$$

$$\Sigma_{es}(u') J(u') \doteq \Sigma_{es}(u) J(u) + (u' - u) \frac{d}{du} [\Sigma_{es}(u) J(u)] \qquad (18b)$$

Substitute equations (18a) into (11a) and (16a) and equation (18b) into (11b) and (16b). Then, evaluating the various integrals over lethargy of $P_0(u-u')$ and $P_1(u-u')$ and eliminating the terms involving $\frac{d}{du}\left[\Sigma_{es}(u)\varphi(u)\right]$ and $\frac{d}{du}\left[\Sigma_{es}(u)J(u)\right]$ result in

$$\gamma(u)\frac{dQ(u)}{du} + Q(u) = \xi_1(u)\Sigma_{es}(u)\varphi(u) \tag{19a}$$

$$\rho(u)\frac{dP(u)}{du} + P(u) = \mu_1(u)\Sigma_{es}(u)J(u) \tag{19b}$$

The parameters appearing in equations (19a) and (19b) are defined, in terms of the quantity $t = u-u'$, as averages over the distribution function $P_0(t)$. That is,

$$\xi_1 \equiv \overline{t} \tag{20a}$$

$$2\xi_1\gamma \equiv \overline{t^2} \tag{20b}$$

$$\mu_1 \equiv \overline{t\mu_L(t)} \tag{20c}$$

$$2\mu_1\rho \equiv \overline{t^2\mu_L(t)} \tag{20d}$$

where the bar denotes an average value. Of course, the various parameters defined by equation (20) depend on lethargy since $P_0(u-u')$ and $P_1(u-u')$ depend upon $f_1(u)$.

Thus, equations (17a), (17b), (19a), and (19b) form the four coupled first-order ordinary differential equations describing the neutron slowing-down process in the consistent P1 approximation to the Boltzmann transport equation. Included are the effects of linearly anisotropic center of mass elastic scattering, inelastic neutron scattering, and lethargy-dependent geometric buckling. Although equations (17) and (19) apply for only one nuclear specie, the extension of the equations to include additional nuclear species follows directly. In particular a set of equations (19) is written for each element with appropriate modifications of equations (17).

Comparison of Lethargy-Dependent Consistent P1 Equations

With Various Approximate Theories

Equations (17) and (19) are fairly general, and it is worth noting that under various restrictions simpler sets of equations, which have been used frequently in reactor analysis, can be easily obtained. This

will be done for a few typical cases. The first of these is the age-diffusion equation with no inelastic scattering which can be obtained from (17) and (19) by setting $\Sigma_{in}(u) \equiv 0$ in (17a), $dP(u)/du \equiv 0$ in (17b), $dQ(u)/du = 0$ in (19a), and $dP(u)/du = P(u) = 0$ in equation (19b).

The familiar Fermi age-diffusion equations result and are given as (ref. 14)

$$B_m(u)J(u) + \Sigma_a(u)\varphi(u) + \frac{dQ(u)}{du} = \frac{f(u)}{K_{eff}} \int_0^\infty du' \nu(u')\Sigma_f(u')\varphi(u') \quad (21a)$$

$$J(u) = D(u)B_m(u)\varphi(u) \quad (21b)$$

$$Q(u) = \xi_1(u)\Sigma_{es}(u)\varphi(u) \quad (21c)$$

where the diffusion coefficient $D(u)$ has been defined as

$$D(u) = \frac{1}{3\{\Sigma_a(u) + \Sigma_{es}(u)[1 - \mu_0(u)]\}} \quad (22)$$

The Selengut-Goertzel approximation is basically the age-diffusion set given by equations (21a) to (21c) but with the element hydrogen treated by equation (19a) - other elements still being treated by equation (21c). To see this, recall that hydrogen exhibits isotropic center of mass elastic scattering collisions over energies of interest in reactors. Thus, $\xi_1(u)$ and $\gamma(u)$ for hydrogen are both equal to unity for all lethargies giving

$$\frac{dQ^H(u)}{du} + Q^H(u) = \Sigma_{es}^H(u)\varphi(u) \quad (23)$$

which is the Selengut-Goertzel equation relating the hydrogen slowing-down density $Q^H(u)$ to the lethargy-dependent flux $\varphi(u)$ (p. 348, ref. 15). The Greuling-Goertzel approximation (p. 390, ref. 15) includes both equations (21a) and (21b) of the age-diffusion formalism but retains equation (19a) for all elements. Other approximations are also possible but will not be discussed because machine programs are just as easily formulated for the basic set of equations given by (17) and (19) as for even the simple age-diffusion set of equations.

Equations for Thermal Group

The slowing-down equations given by (17a), (17b), (19a), and (19b) are assumed to apply to some cutoff lethargy u_T corresponding to an energy E_T. The energy E_T is usually taken as about $5kT$ where T is the temperature of the moderator in $^\circ K$ and k is the Boltzmann constant. In the energy range from 0 to E_T the neutrons have energies

comparable to the energies of the thermally agitated nuclei and can gain as well as lose energy upon making a collision. However, if the absorption and leakage of neutrons are small, the neutron energy spectrum will approach a Maxwell-Boltzmann distribution in speed with a temperature corresponding to that of the moderator. Under these conditions and using the principle of detailed balance, the thermal equation in the P1 approximation will be, after separating the spatial function as before,

$$B_{m_T} J_T + \Sigma_{a_T} \varphi_T = Q(u_T) + \int_{u_T}^{\infty} du \int_{-\infty}^{u_T} du' \Sigma_{in}(u') \varphi(u') H(u' \to u) \quad (24a)$$

$$-\frac{1}{3} B_{m_T} \varphi_T + \Sigma_{tr_T} J_T = P(u_T) \quad (24b)$$

where Σ_{a_T} and Σ_{tr_T} are the appropriate averaged values of the macroscopic absorption and transport cross sections over the thermal speed range. Thus, equations (17a), (17b), (19a), (19b), (24a), and (24b) form the complete set of consistent P1 equations extended to include many elements, which are the basis for an IBM 704 code.

Discussion of Boundary Conditions, Fission Spectrum,

and Inelastic Scattering Kernel

If the zero of lethargy is taken sufficiently lower than the lowest lethargy in the source spectrum, the initial conditions for the set of consistent P1 equations will be

$$Q(u=0) = 0, \quad \varphi(u=0) = 0 \quad (25a)$$

$$P(u=0) = 0, \quad J(u=0) = 0 \quad (25b)$$

Depending upon the reactor, a number of possible source spectrums can be used. For this study the uranium-235 fission spectrum, given in analytic form as

$$f(u) = 0.45270 \, E \, \exp\left(\frac{-E}{0.965}\right) \sinh\sqrt{2.29 \, E} \quad (26)$$

has been used. The quantity E is the neutron energy in Mev. The spectrum is normalized to unity; that is,

$$\int_0^{\infty} du \, f(u) = 1.0 \quad (27)$$

This normalization of the source spectrum permits the evaluation of the static criticality factor of the reactor as

$$K_{eff} = \int_0^\infty du \nu(u) \Sigma_f(u) \varphi(u) \tag{28}$$

The characteristic dimension of the reactor is needed to compute the lethargy-dependent buckling $B_m(u)$. For example, in the case of a spherical reactor the equation used for $B_m(u)$ is

$$B_m(u) = \frac{\pi}{r + 0.71 \lambda_{tr}(u)} \tag{29}$$

where r is the radius and where

$$\lambda_{tr}(u) = 3D(u) \tag{30}$$

The inelastic scattering kernel in equation (17a) has been obtained from the evaporation model of the nucleus as described by Blatt and Weisskopf (ref. 16). The evaporation model of the nucleus appears to give the gross features of heavy element inelastic scattering. In terms of energy, this model gives for the inelastic kernel the following result:

$$H(E' \rightarrow E) = const. \ E\left[e^{-\zeta(E')E}\right] \tag{31}$$

where the constant is determined from the normalization requirement that

$$\int_0^{E'} dE \ H(E' \rightarrow E) = 1.0 \tag{32}$$

In equation (31) E' represents the initial energy of the neutron and E the energy after an inelastic scattering collision has occurred. The quantity $\zeta(E')$ is the reciprocal nuclear temperature in Mev^{-1} and is a function of the scattering nucleus and initial energy of the neutron. It has been approximated by

$$\zeta(E') = \left(\frac{a}{4E'}\right)^{1/2} \tag{33}$$

with the parameter a being experimentally determined for each nucleus of interest.

Discussion of Neutron Cross Sections

The lethargy-dependent consistent Pl equations described along with the initial conditions, source spectrum, and approximate inelastic scattering kernel are integrated for a homogeneous unreflected reactor system over the microscopic cross-section data of the elements involved

in a stepwise fashion from 10^7 ev to 0.025 ev (or from lethargy u = 0
to u = 19.8). This lethargy range is spanned by 473 mesh points such
that the cross sections of the various elements are well represented
in the resonance energy range. The microscopic cross-section data of
29 elements are represented in such a fashion for use with the IBM 704
code. These cross-section data include σ_a, σ_{es}, $\nu\sigma_f$, f_1, and σ_{in}
where σ_a is the microscopic absorption cross section, σ_{es} is the
microscopic elastic scattering cross section, $\nu\sigma_f$ is the microscopic
production cross section, f_1 is the average cosine of the angle between
the initial and final direction of motion of an elastically scattered
neutron as measured in the center of mass coordinate system, and σ_{in}
is the microscopic inelastic scattering cross section. The quantity ν
is the average number of neutrons produced in fission, and σ_f is the
microscopic fission cross section. The quantity ν is taken to be
energy-dependent according to the data of reference 17. In the thermal
energy range the absorption and fission cross sections are corrected for
non-1/v behavior as well as for hardening of the thermal spectrum, due
to absorption, using the data of reference 18. The transport cross sec-
tion at thermal energy is similarly corrected.

THEORETICAL RESULTS AND COMPARISON WITH EXPERIMENT

Age of Fission Neutrons in Water

One of the important parameters describing moderating materials is
the fission neutron age τ. For hydrogenous media the age becomes espe-
cially important because of the well-known discrepancy for water between
the experimental measurements and various theoretical calculations. For
any homogeneous medium the lethargy-dependent consistent P1 equations
can be solved for a given set of microscopic cross-section data, the
uranium-235 fission spectrum, and for a constant buckling B_m. From
the neutron fluxes and currents generated as a function of lethargy, it
is possible to compute the weighted fission age.

In this work, the weighted fission age for water to indium reso-
nance energy is computed to be 26.5 square centimeters. Oxygen was con-
sidered to have linearly anisotropic center of mass elastic scattering.
For isotropic center of mass scattering for oxygen, the age is calcu-
lated to be 24.7 square centimeters. This demonstrates the importance
of precise calculation of the various competing effects on the neutron
spectrum. For comparison of the age of 26.5 square centimeters calcu-
lated in this work, the weighted mean of a number of different types of
calculations is given in reference 19 as 26.0±0.5 square centimeters.
It is also of interest to note that a recent measurement of the fission
neutron age in water is 27.86 square centimeters (ref. 20).

E-690

Fourier Transform of Slowing-Down Kernel in Water

Another important property of homogeneous moderating media can be described in terms of the Fourier transform $\overline{K}(B_m)$ of the slowing-down kernel. Physically, the Fourier transform $\overline{K}(B_m)$ is the nonleakage probability of the source neutrons to a given energy. The transform $\overline{K}(B_m)$ can be derived from a solution of the lethargy-dependent consistent P1 equations for a given source spectrum and a constant value of the buckling B_m.

Figure 1 is a plot of the transform $\overline{K}(B_m)$ as a function of B_m for fission neutrons in water to indium resonance energy. Shown on the curve are values of the transform computed by Gwin, Trubey, and Weinberg (fig. 1, ref. 6) from the experimental slowing-down kernel as measured by Hill, Roberts, and Fitch (ref. 21). The agreement over a wide range of buckling is seen to be good. The value of the fission neutron age in water reported in reference 21 is higher than the recent value of reference 20 by about 3 square centimeters. This is believed due to differences between the two experiments of measurements near the source. This difference near the source of the reference 21 measurement of the slowing-down kernel in water is expected to have a small effect on the calculation of the transform $\overline{K}(B_m)$.

Table I compares the transform $\overline{K}(B_m)$ to indium resonance energy for water and two concentrations of uranyl fluoride salt in water solution. The differences as compared to water are slight except for extreme values of the buckling.

Calculation of Critical Dimensions of Unreflected

Homogeneous UO_2F_2-H_2O Assemblies

The lethargy-dependent equations of the consistent P1 slowing-down model described in the section on theory will be used to calculate the parameters of critical assemblies of unreflected uranyl fluoride salt UO_2F_2 dissolved in water. Comparison of theoretical results with available experimental data will also be made.

Before any calculations can be performed, the physical properties of uranyl fluoride - water solutions must be known. Figure 2 is a curve of density of uranyl fluoride - water solutions as a function of hydrogen atom concentration for a temperature of 25° C obtained from available experimental data (ref. 22). The point on the curve for pure water is for a density of 0.997 gram per cubic centimeter and a hydrogen atom concentration of 6.66×10^{22} atoms per cubic centimeter. Since the uranium in the solution is considered to contain 93.2 percent by weight of the

uranium-235 isotope, the data of figure 2 can be used to derive a curve, figure 3, of the uranium-235 atom concentrations N^{25} in atoms per cubic centimeter as a function of the hydrogen atom concentration N^H in atoms per cubic centimeter. On figure 3 are also indicated various values of R defined to be the ratio of the hydrogen atom concentration to uranium-235 atom concentration, $R = N^H/N^{25}$. Various important characteristics of the UO_2F_2-H_2O critical assemblies will be given in terms of this parameter R.

Thus, specification of the solution density for the UO_2F_2-H_2O solution reactor in question gives the hydrogen atom concentration from the curve given by figure 2. Then, from figure 3 the uranium-235 concentration can be determined. The atom densities for the other constituents of the solution are determined from the following relations:

$$\text{Uranium-238:} \quad N^{28} = 0.0730 \ N^{25} \qquad (34a)$$

$$\text{Fluorine:} \quad N^F = 2(N^{25} + N^{28}) \qquad (34b)$$

$$\text{Oxygen:} \quad N^{O2} = \frac{1}{2} N^H + N^F \qquad (34c)$$

By using the atom concentration for the various constitutents of the UO_2F_2-H_2O solutions in the manner described, calculations were performed, using the lethargy-dependent consistent P1 equations over the 473 lethargy points of the microscopic cross-section data extending from 10^7 ev to 0.025 ev, over a wide range of solution concentrations. In terms of the parameter R, the solution concentrations were varied from R = 25 to 700. As a result of these many calculations, the static criticality factor K_{eff} is obtained for a given hydrogen to uranium-235 atom concentration (R) as a function of the buckling B_m^2 of the system. The buckling, although capable of being varied with the lethargy in the IBM 704 code, was considered to be lethargy-independent for these calculations.

As examples, the lethargy-dependent flux $\varphi(u)$ is plotted as a function of lethargy u for critical reactors having solution concentration values of R = 40 and 472. The source term for the calculations corresponds to 1 fission neutron. The flux for R = 40, a system heavily loaded with uranium-235, is shown in figure 4. In the fission spectrum lethargy range from about lethargy u = 0 to u = 6 a resonance structure in the flux is noted which corresponds to various high-energy scattering resonances of oxygen. In the resonance energy range from lethargy u = 6 to u = 18.2, the decrease in the flux with lethargy occurs because of the absorption by the uranium-235 nuclei. The dips in the flux correspond to absorption resonances in the uranium-235. The effect on the flux of the approximately 1/v capture is

evident from lethargy u = 15.0 to 18.2. The flux for R = 472, a
system lightly loaded with uranium-235, is shown in figure 5. In the
lethargy range from u = 0 to 6 the flux for R = 472 appears roughly
the same as for the R = 40 system. In the lethargy range from u = 6
to u = 18.2 the flux is constant from about lethargy u = 7 to
u = 12.0. From lethargy u = 12.0 to 18.2 the effects of uranium-235
absorption resonances and 1/v capture are evident but are not as
drastic as for the heavily loaded R = 40 reactor system.

Figure 6 is a plot of the static criticality factor K_{eff} for un-
reflected UO_2F_2-H_2O assemblies as a function of the parametric R and
the buckling B_m^2. Curves of the criticality factor varying from 0.98
to 1.12 are shown. All the curves exhibit a broad minimum in the buck-
ling over values of R from 40 to 70. For the static criticality
factor equal to unity the radius of the equivalent unreflected sphere,
which includes the extrapolation distance, varies from about 18.25 to
25 centimeters over the range of the parameter R.

<div style="text-align:center">Comparison of Calculated Critical Dimensions with Experimental</div>

<div style="text-align:center">Values for Unreflected UO_2F_2-H_2O Assemblies</div>

In order to compare calculated critical dimensions with experi-
mentally determined values, the effect of the aluminum containment
vessels on measured critical dimensions of unreflected UO_2F_2-H_2O assem-
blies must be known. The worth of the aluminum bottom plate for the
NASA experiments was measured in terms of the change in critical height
as a function of the thickness of the bottom plate for a 12-inch-
diameter cylindrical tank. The solution concentration R was 475.
These results are shown in figure 7 where it is seen that, for example,
a 1-centimeter-thick bottom plate is worth about 0.3 centimeter of solu-
tion height for this particular reactor. It is expected that the bottom
plate worths for other values of R would be nearly the same as for the
values for R = 475 since the fraction and spectrum of neutrons leaking
from these do not differ greatly. It is estimated that the reported
critical height for the NASA experiments could be too low by a maximum
of about 0.5 centimeter since the wall thickness of the aluminum cylinder
is 1/8 inch. Thus, because of the expected smallness of this correction,
none of the Oak Ridge and NASA criticality data have been corrected for
the criticality effect of the aluminum containment vessels.

Since figure 6 is based on an energy-independent buckling, this
implies an energy-independent extrapolation distance δ. This value of
δ can be deduced from experimental criticality data on unreflected
cylinders if the top, bottom, and side extrapolation distances are
assumed to be equal. Then, comparison with a wide range of reactor

dimensions and solution concentrations will establish the validity of a constant value for δ. Figure 8 shows theoretical curves based on values of δ = 2.5, 3.0, and 3.5 centimeters for unreflected 12-inch-diameter cylindrical reactors of UO_2F_2-H_2O solution in which the critical height is plotted as a function of the parameter R. These curves are based on the following equation for the critical height h of the cylinders:

$$h = \sqrt{\frac{\pi^2}{B_z^2}} - 2\delta \tag{35a}$$

where

$$B_z^2 = B_m^2 - \left(\frac{2.4048}{r + \delta}\right)^2 \tag{35b}$$

and r is the physical radius of the cylinders. For a given value of R, B_m^2 is evaluated from figure 6 for a K_{eff} of unity, and then, since the values of r and δ have been fixed, the physical height h is given by equations (35a) and (35b). It is evident from figure 8 that these critical assemblies are quite sensitive to the value of the extrapolation distance which is used. For the 12-inch-diameter cylindrical reactors considered the value of δ = 3.0 centimeters seems to predict the experimental critical heights listed in table II quite well as a function of the atom ratio parameter R. This insensitivity of δ with R is probably due to the fact that the hydrogen atom density, and hence the leakage fraction, changes but little over the range of R considered. Therefore, it was decided to use this value of δ = 3.0 centimeters for the extrapolation distance for all values of the parameter R for the various diameters of the unreflected cylindrical critical assemblies of UO_2F_2-H_2O. Reference 6 reports using values of δ = 2.5 to 3.7 for the empirical kernel method of calculation.

The curves of figure 9 represent calculations of the critical heights of cylindrical reactors for various diameters and as a function of the parameter R. These calculations are based on the theoretical buckling curve given as figure 6 and the assumed constant value of the extrapolation distance δ = 3.0 centimeters. The experimental points, listed in table II, represent data from references 2, 3, 4, and the NASA solution reactor. The agreement for various diameter reactors as a function of R is quite good between the theoretical model described in this work and the various experiments. Thus, this provides the verification of the general buckling curve (fig. 6) and of the constant value of 3.0 centimeters for the extrapolation distance for these unreflected cylindrical reactors.

Calculation of Nonthermal Fission Fractions, Leakage Fractions,

Neutron Age, and Two- and Three-Group Macroscopic Cross

Sections as a Function of Solution Concentration

for UO_2F_2-H_2O Assemblies

In solving for the critical dimensions of unreflected UO_2F_2-H_2O reactors using the consistent P1 equations, the lethargy-dependent flux $\varphi(u)$ and current $J(u)$ are generated. Since all the information about a given reactor is contained by the flux and current, it is possible to derive many useful quantities pertaining to the UO_2F_2-H_2O reactors. Figures 10, 11, and 12 present some of this information.

In figure 10 is plotted the nonthermal fission fraction as a function of the parameter R for various cutoff energies. For a heavily loaded UO_2F_2-H_2O system having $R = 25$, about 65 percent of the nonthermal fissions occur between energies of 10^7 ev to 0.125 ev, while about 43 percent of the total fissions occur between energies of 10^7 ev to 1.44 ev. For a UO_2F_2-H_2O reactor having $R = 700$ the corresponding numbers are about 6 and 3 percent.

Figure 11 is a plot of the fraction of the neutrons which escape from critical UO_2F_2-H_2O systems as a function of R. This fraction is nearly constant over the range of R from 25 to about 300, varying between 44 and 47 percent. For larger values of R this function decreases and is about 33 percent at $R = 700$.

Figure 12 is a plot of the fission neutron age τ as a function of the parameter R both for the indium resonance detector energy of 1.44 ev and the thermal cutoff energy of 0.125 ev. From about $R = 100$ to $R = 700$ the age is nearly constant. For values of R less than 100 the age increases because of the decreased hydrogen atom concentration. In the limit as $R \rightarrow \infty$ the 1.44-ev curve would approach the fission neutron age in water.

The neutron fluxes generated in solving for the critical dimensions of unreflected UO_2F_2-H_2O systems can also be used as a weighting function for obtaining two- and three-group macroscopic cross-section parameters. These two- and three-group cross sections can be used in calculating reflected UO_2F_2-H_2O solution reactors.

Both three- and two-group constants were generated as a function of
R.   Group I of the three-group split extends from   u = 0   to   u = 6.1,
group II from   u = 6.1   to   u = 18.2,   and the thermal group is centered
about the lethargy of 19.8 corresponding to the room temperature   kT   of
0.025 ev.   For the two-group split, the thermal group is the same as
that of the three-group split, and the fast group (group I) extends from
lethargy   u = 0   to   u = 18.2.   For the few-group calculations performed
with a one-dimensional multigroup IBM 704 code, the parameters needed
are the group diffusion coefficient D^G, group macroscopic absorption
cross section Σ_a^G, group macroscopic production cross section $\nu\Sigma_f^G$, and
the group removal cross section Σ_q^G.   These group parameters are defined
over the fluxes and currents generated for a given value of   R   as

$$D^G = \frac{\displaystyle\int_{group} J(u)du}{\displaystyle\int_{group} B_m(u)\varphi(u)du} \tag{36a}$$

$$\Sigma_a^G = \frac{\displaystyle\int_{group} \Sigma_a(u)\varphi(u)du}{\displaystyle\int_{group} \varphi(u)du} \tag{36b}$$

$$\nu\Sigma_f^G = \frac{\displaystyle\int_{group} \nu(u)\Sigma_f(u)\varphi(u)du}{\displaystyle\int_{group} \varphi(u)du} \tag{36c}$$

The quantity Σ_q^G is evaluated by making a neutron balance over the
group in question.   Over the range of buckling considered, the group
constants were not sensitive to the choice of buckling B_m.

The few-group constants obtained by the method described are shown
in figures 13, 14, 15, and 16 for both the three- and two-group splits
over the range of   R   values.   The diffusion coefficient   D   is plotted
in figure 13 and is relatively constant over the entire range of   R   for
most of the fast groups; however, the effect of uranium-235 absorption
is seen for all the   R   values for the thermal neutron group.   The ab-
sorption cross section Σ_a^G is shown in figure 14 and varies strongly
with the atom ratio   R.   The production cross section $\nu\Sigma_f^G$ is shown in
figure 15 and exhibits similar behavior as the absorption cross section.
The removal cross section Σ_q is shown in figure 16 and increases as

the parameter R increases. Table III gives the corresponding three-
and two-group data for water at room temperature.

Comparison of Calculated and Experimental Critical Dimensions

for Water-Reflected UO_2F_2-H_2O Reactors

In order to perform theoretical calculations on fully reflected
cylinders, the reflector savings must be established as a function of
reflector thickness and concentration parameter R. Using the three-
group parameters plotted in figures 13 to 16 for various values of R
and the water constants listed in table III, the critical core radius r
was calculated for spherical reactors of UO_2F_2-H_2O solutions with various
thicknesses of water using an IBM 704 diffusion code. The reflector
savings RS is defined as

$$RS = \sqrt{\frac{\pi^2}{B_m^2}} - r \tag{37}$$

where for a given value of R the value of B_m^2 is obtained from fig-
ure 6. The results of these calculations are shown in figure 17. The
curves show a slight increase in the reflector savings with R. For the
completely reflected case (60 cm of water) the value of reflector savings
is 5.5 centimeters at R = 25 and 6.0 centimeters at R = 700. For the
range of R values considered the reflector savings reached its maximum
value at about 15 centimeters thickness of water.

The critical heights h of fully reflected cylindrical assemblies
were computed for cores of radius r as a function of the parameter R
using the critical buckling curve of figure 6 and the infinite water
reflector savings curve of figure 17. These results are shown in fig-
ure 18 and were calculated with the following two formulas:

$$h = \sqrt{\frac{\pi^2}{B_z^2}} - 2RS \tag{38a}$$

$$B_z^2 = B_m^2 - \left(\frac{2.4048}{r + RS}\right)^2 \tag{38b}$$

Experimentally obtained data listed in table IV are also shown on the
curves. The agreement is generally good. The dashed curves were com-
puted by arbitrarily increasing the reflector savings by 0.5 centimeter
for all values of R. The two sets of curves bracket the experimental
data quite well and serve to indicate the sensitivity of the calculations
with small changes in the value of the reflector savings.

CONCLUSION

The lethargy-dependent equations of the consistent P1 approxima-
tion to the Boltzmann transport equation for slowing down neutrons, as
developed in this present study, have been used as the basis of an IBM
704 computer program. This program has been used to compute the age of
fission neutrons in water as 26.5 square centimeters as compared to a
recent experimental value given as 27.86 square centimeters. The
Fourier transform of the slowing-down kernel for water to indium reso-
nance energy calculated here compares well with the Fourier transform of
the kernel for water measured by Hill, Roberts, and Fitch. This method
of calculation has also been applied to uranyl fluoride - water solution
critical assemblies. Theoretical results established for both unre-
flected and fully reflected critical assemblies compare well with avail-
able experimental data.

Lewis Research Center
    National Aeronautics and Space Administration
        Cleveland, Ohio, August 22, 1961

E-690

APPENDIX - SYMBOLS

A	ratio of nuclear mass to neutron mass
a	inelastic scattering parameter defined by eq. (33)
$B_m(u)$	lethargy-dependent material buckling defined by eqs. (8) and (9)
B_z^2	transverse buckling for cylindrical geometry
$D(u)$	diffusion coefficient at lethargy u defined by eq. (22), cm
D^G	neutron diffusion coefficient for group G defined by eq. (36a), cm
$d\vec{r}$	spatial volume element
du	element of lethargy
$d\vec{v}$	velocity volume element
E	neutron energy
E_T	thermal cutoff energy separating thermal energy range from fast energy range
F	spatial function defined by eq. (8b)
$f(u)du$	fraction of source neutrons in lethargy interval du about lethargy u
$f_1(u)$	average cosine of angle between initial and final direction of motion, measured in the center of mass coordinate system, for elastically scattered neutrons of lethargy u
G	spatial function defined by eq. (8a)
$H(\vec{v}' \rightarrow \vec{v})d\vec{r}\,d\vec{v}$	probability that a neutron in phase volume element $(d\vec{r}\,d\vec{v}')$ will, after an inelastic scattering collision, be in the phase volume $(d\vec{r}\,d\vec{v})$
h	physical height of cylindrical reactor
$J(u)$	lethargy-dependent neutron current defined by eq. (17b)

$\overline{K}(B_m)$ Fourier transform of neutron slowing-down kernel

K_{eff} static criticality factor for a reactor

k   Boltzmann constant

N   concentration of an element, atoms/cm^3

$n(\vec{r},\vec{v})d\vec{r}\,d\vec{v}$ probable number of neutrons in space volume element $d\vec{r}$ about position $\vec{r}$ and in velocity element $d\vec{v}$ about velocity $\vec{v}$ per unit time

$P(u)$ anisotropic slowing-down density defined by eq. (19b)

$P(\vec{v}'\rightarrow\vec{v})d\vec{r}\,d\vec{v}$ probability that a neutron in the phase volume element $(d\vec{r}\,d\vec{v}')$ will, after an elastic scattering collision, be in the phase volume $(d\vec{r}\,d\vec{v})$

$P_l(u-u')$ lethargy-dependent coefficient of index l, in expansion of elastic scattering kernel into a series of Legendre polynomials, defined by eq. (13)

$P_l(\mu)$ Legendre polynomial or argument μ and index l

$Q(\vec{r},u,\vec{\Omega})$ slowing-down density defined as number of elastic scattered neutrons which pass lethargy mark u per unit time per unit phase volume $(d\vec{r}\,d\Omega)$

$Q(u)$ isotropic slowing-down density defined by eq. (19a)

$Q_l(Z,u)$ coefficient of index l in expansion of slowing-down density into a series of Legendre polynomials defined by eq. (7)

R   ratio of hydrogen atom concentration to uranium atom concentration for the UO_2F_2-H_2O solution reactors

RS   reflector savings defined by eq. (37)

r   physical radius of cylindrical reactors

$\vec{r}$ position vector

$S(\vec{r},\vec{v})d\vec{r}\,d\vec{v}$ source of neutrons due to fission which are produced in phase volume element $(d\vec{r}\,d\vec{v})$

T   moderator temperature, $°K$

t	contraction for lethargy difference $u-u'$
u	neutron lethargy defined in terms of neutron energy E by equation $u = \ln(E_0/E)$, E_0 usually taken as 10^7 ev
u_T	cutoff lethargy corresponding to cutoff energy E_T
v	neutron speed corresponding to energy E
$\vec{v}$	neutron velocity
Z	coordinate axis
γ	quantity related to mean squared lethargy increase per collision, defined by eq. (20b)
δ	Dirac delta function used in eq. (12)
δ	extrapolation distance defined by eqs. (35a) and (35b)
$\delta_{0,l}$	Kronecker delta defined by eq. (5)
ζ	reciprocal nuclear temperature defined by eq. (33)
λ_{tr}	neutron transport mean free path defined by eq. (30)
μ	cosine of angle between Z-axis and direction of motion of neutron in planar geometry
μ_L	cosine of angle between initial and final directions of motion measured in laboratory coordinate system of a neutron undergoing an elastic scattering collision
μ_0	average cosine, measured in laboratory coordinate system, for elastically scattered neutrons
μ_1	mean of the product of lethargy increase in a collision times angle of scattering, defined by eq. (20c)
$\nu(E)$	average number of neutrons produced per fission occurring at energy E
ξ_1	average increase in lethargy per collision
ρ	quantity related to mean of the product of squared lethargy increase per collision times angle of scattering, defined by eq. (20d)

Σ_a — macroscopic neutron absorption cross section, cm^{-1}

Σ_{es} — macroscopic neutron elastic scattering cross section, cm^{-1}

Σ_f — macroscopic neutron fission cross section, cm^{-1}

Σ_{in} — macroscopic neutron inelastic scattering cross section, cm^{-1}

Σ_t — macroscopic neutron total cross section, $\Sigma_a + \Sigma_{es} + \Sigma_{in}$, cm^{-1}

Σ_a^G — macroscopic neutron absorption cross section for group G, defined by eq. (36b), cm^{-1}

Σ_f^G — macroscopic neutron fission cross section for group G, defined by eq. (36c), cm^{-1}

Σ_q^G — macroscopic neutron removal cross section for group G, cm^{-1}

σ_a — microscopic neutron absorption cross section, cm^2

σ_{es} — microscopic neutron elastic scattering cross section, cm^2

σ_f — microscopic neutron fission cross section, cm^2

σ_{in} — microscopic neutron inelastic scattering process, cm^2

$\tau(E',E)$ — neutron age, defined as one-sixth the mean squared slowing-down distance to energy E of a neutron originating from a point source emitting neutrons of energy E' in an infinite medium

φ — neutron flux, nv

$\vec{\Omega}$ — unit vector in direction of motion of neutron

REFERENCES

1. Lewis Flight Propulsion Laboratory Staff: NACA Zero Power Facility Hazards Summary. NACA RM E57F28, 1957.

2. Beck, C. K., Callihan, A. D., Morfitt, J. W., and Murray, R. L.: Critical Mass Studies, pt. III. Rep. K-343, K-25 Plant, Carbide and Carbon Chem. Corp., Apr. 19, 1949.

3. Fox, J. K., Gilley, L. W., and Callihan, A. D.: Critical Mass Studies. Pt. IX - Aqueous U-235 Solutions. ORNL-2367, Oak Ridge Nat. Lab., Mar. 4, 1958.

4. Fox, J. K., and Gilley, L. W.: Critical Parameters of Aqueous Solutions of U-235. Applied Nuclear Division - Annual Progress Report for Period Ending Sept. 1, 1957. ORNL-2389, Oak Ridge Nat. Lab., Nov. 26, 1957, pp. 71-83.

5. Callihan, Dixon: Homogeneous Critical Assemblies. Vol. 1 - Physics and Mathematics. Progress in Nuclear Energy, McGraw-Hill Book Co., Inc., 1956, pp. 227-250.

6. Gwin, R., Trubey, D. K., and Weinberg, A. M.: Experimental and Theoretical Studies of Unreflected Aqueous U-235 Critical Assemblies. Vol. 12 - Reactor Physics. Proc. Second United Nations Int. Conf. on Peaceful Uses of Atomic Energy, 1958, pp. 529-538.

7. Mills, C. B.: Minimum Critical Dimensions for Water Solutions. Nuclear Sci. and Eng., vol. 9, no. 3, Mar. 1961, pp. 377-390.

8. Hughes, Donald J., and Schwartz, Robert B.: Neutron Cross Sections. BNL-325, Second ed., Brookhaven Nat. Lab., July 1, 1958. (See also Supplement 1, Second ed., Jan. 1, 1960.)

9. Howerton, Robert J.: Semi-Empirical Neutron Cross Sections. Pt. II, vol. 1 - 0.5 - 15.0 MEV. UCRL-5351, Univ. Calif., 1958.

10. Hughes, Donald J., and Carter, Robert S.: Neutron Cross Sections - Angular Distributions. BNL-400, AEC, June 1956.

11. Davison, B.: Neutron Transport Theory. Clarendon Press (Oxford), 1957.

12. Simon, A.: Neutron Slowing Down by Hydrogen in the Consistent P1 Approximation. ORNL-2098, Oak Ridge Nat. Lab., July 5, 1956.

13. Marshak, Robert E.: Theory of the Slowing Down of Neutrons by Elastic Collision with Atomic Nuclei. Rev. Modern Phys., vol. 19, no. 3, July 1947, pp. 185-238.

14. Weinberg, Alvin M., and Wigner, Eugene P.: The Physical Theory of Neutron Chain Reactors. Univ. Chicago Press, 1958, ch. 11.

15. Hurwitz, H., Jr., and Ehrlich, R.: Highly Enriched Intermediate and Thermal Assemblies. Vol. 1 - Physics and Mathematics. Progress in Nuclear Energy, McGraw-Hill Book Co., Inc., 1956, pp. 343-392.

E-390

28

16. Blatt, John M., and Weisskopf, V. F.: Theoretical Nuclear Physics.
    John Wiley & Sons, Inc., 1952.

17. Anon.: Reactor Physics Constants. ANL-5800, Argonne Nat. Lab.,
    1958, p. 3.

18. Amster, Harvey J.: A Compendium of Thermal Neutron Cross Sections
    Averaged over the Spectra of Wigner and Wilkens. WAPD-185, Bettis
    Plant, Westinghouse Electric Corp., Jan. 1958.

19. Goldstein, Herbert, Zweifel, P. F., and Foster, D. G., Jr.: The
    Slowing Down of Neutrons in Hydrogenous Media - Status of Theory
    and Experiment. Vol. 16 - Nuclear Data and Reactor Theory.
    Second United Nations Int. Conf. on Peaceful Uses of Atomic Energy,
    1958, pp. 379-404.

20. Doerner, R. C., Armani, R. J., Zagotta, W. E., and Martens, F. H.:
    Age of Fission Energy Neutrons to Indium Resonance in Water.
    Nuclear Sci. and Eng., vol. 9, no. 2, Feb. 1961, pp. 221-240.

21. Hill, J. E., Roberts, L. D., and Fitch, T. E.: Slowing Down Dis-
    tribution of U-235 Fission Neutrons from a Point Source in Light
    Water. Jour. Appl. Phys., vol. 26, no. 8, Aug. 1955, pp. 1013-1017.

22. Hogerton, John F., and Grass, Robert C., eds.: The Reactor Handbook.
    Vol. 2 - Engineering. AECD-3646, AEC, May 1955, pp. 581-593.

TABLE I. - FOURIER TRANSFORM $\overline{K}(B_m)$ OF SLOWING-DOWN

KERNEL FOR FISSION NEUTRONS IN WATER AND IN

UO_2F_2-H_2O SOLUTIONS WITH ATOM RATIOS

OF HYDROGEN TO URANIUM-235, R,

EQUAL TO 50, 150

B_m	$\overline{K}(B_m)$		
	$H_2O(R=\infty)$	$R = 150$	$R = 50$
0	1.0	1.0	1.0
.03142	.9745	.9748	.9752
.06283	.9047	.9057	.9069
.12566	.6944	.6970	.7000
.20944	.4188	.4220	.4263
.26180	.2881	.2922	.2970
.31416	.1923	.1963	.2013
.3927	.0995	.1030	.1079
.5236	.0285	.0310	.0349
.7854	.0005	.0013	.0028

TABLE II. - EXPERIMENTAL CRITICALITY DATA FOR UO_2F_2-H_2O UNREFLECTED

SOLUTION REACTORS CONTAINED BY ALUMINUM VESSELS

Cylinder diameter, in.	Atom ratio, $R = N^H/N^{U-235}$	Critical height, cm	Reference	Cylinder diameter, in.	Atom ratio, $R = N^H/N^{U-235}$	Critical height, cm	Reference
10	52.9	34.0	2, p. 75	15	169.0	18.5	2, p. 75
	169.0	41.2	2, p. 75		328.7	21.7	↓
					499.0	27.4	
	27.1	38.9	3, p. 24		755.0	43.6	
	44.3	35.1	↓				
	73.4	33.7			27.1	18.5	3, P. 25
					44.3	17.9	↓
	43.2	[a]34.9	4, p. 73-74		74.6	16.8	
	44.7	[a]34.7					
	50.1	34.8			50.1	17.9	4, p. 73
	51.5	[a]33.5			331	22.9	4, p. 73
	55.4	34.3					
	60.8	34.1		20	27.1	15.8	3, p. 25
	66.1	34.1			44.3	15.0	↓
	71.5	34.1			73.4	15.2	
	83.1	34.4					
	85.7	34.9			50.1	15.4	4, p. 73
12	44.3	23.2	3, p. 25		60.8	15.3	
					325	18.7	↓
	50.1	22.6	4, p. 73	30	44.3	13.7	3, p. 25
	51.5	22.6			72.4	13.9	3, p. 25
	55.4	[a]22.6					
	60.8	22.7	↓		50.1	13.8	4, p. 73
	331	32.8			51.5	[a]13.3	
					331	16.3	↓
	185	25.3	Present work				
	218	26.6					
	250	28.3					
	253	28.5					
	285	30.2					
	320	32.0					
	365	35.4					
	405	37.0					
	435	43.6					
	455	46.2					
	460	47.0					
	465	48.2					
	485	48.8					

[a]Value too low according to ref. 4.

TABLE III. - THREE- AND TWO-GROUP CONSTANTS FOR WATER REFLECTOR

Lethargy, u	Diffusion coefficient, D^G	Absorption cross section, Σ_a^G	Removal cross section, Σ_q^G
0-18.2	1.274	0.00066	0.04598
0-6.1	1.722	.00012	.07837
6.1-18.2	.612	.00145	.11392
19.8	.1329	.01962	--------

TABLE IV. - EXPERIMENTAL CRITICALITY DATA FOR UO_2F_2-H_2O REACTORS

FULLY REFLECTED BY AN INFINITE WATER REFLECTOR

Cylinder diameter, in.	Atom ratio, $R = N^H/N^{U-235}$	Critical height, cm	Reference
8	26.2	21.5	2, p. 69
	29.9	20.7	
	52.9	19.5	
	58.8	20.5	
	99.5	22.4	
	192.0	28.1	
	290.0	40.1	
	43.2	18.6	4, p. 72
10	52.9	13.4	2, p. 69
	328.7	22.4	
	499	35.2	
	43.2	12.5	4, p. 72
	51.5	11.4	4, p. 72
15	52.9	7.90	2, p. 69
	56.7	8.50	
	221.0	11.30	
	499.0	16.90	
	755.0	27.10	
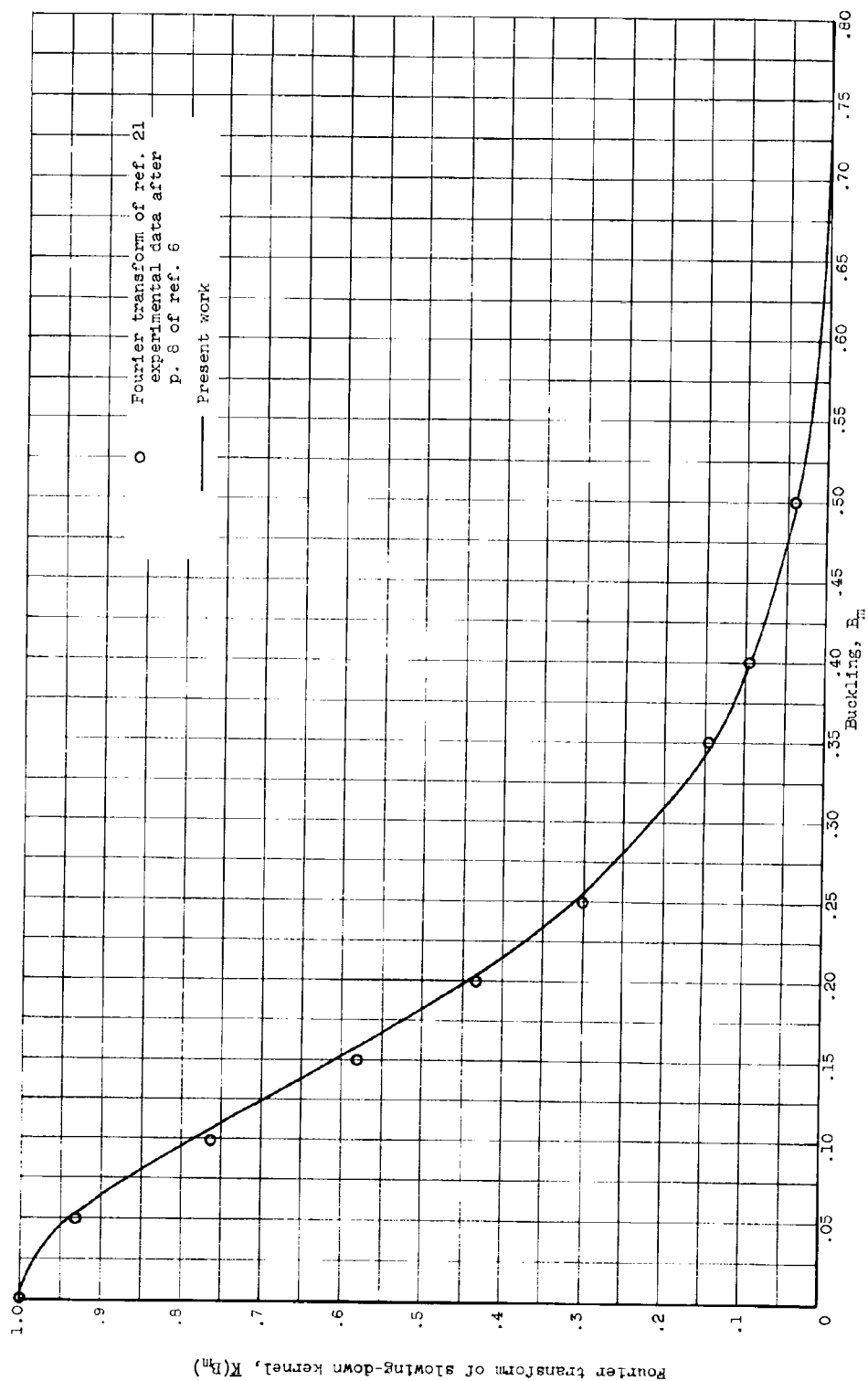
Figure 1. - Fourier transform $\overline{K}(B_m)$ of slowing-down kernel in water to indium resonance energy.

E-690
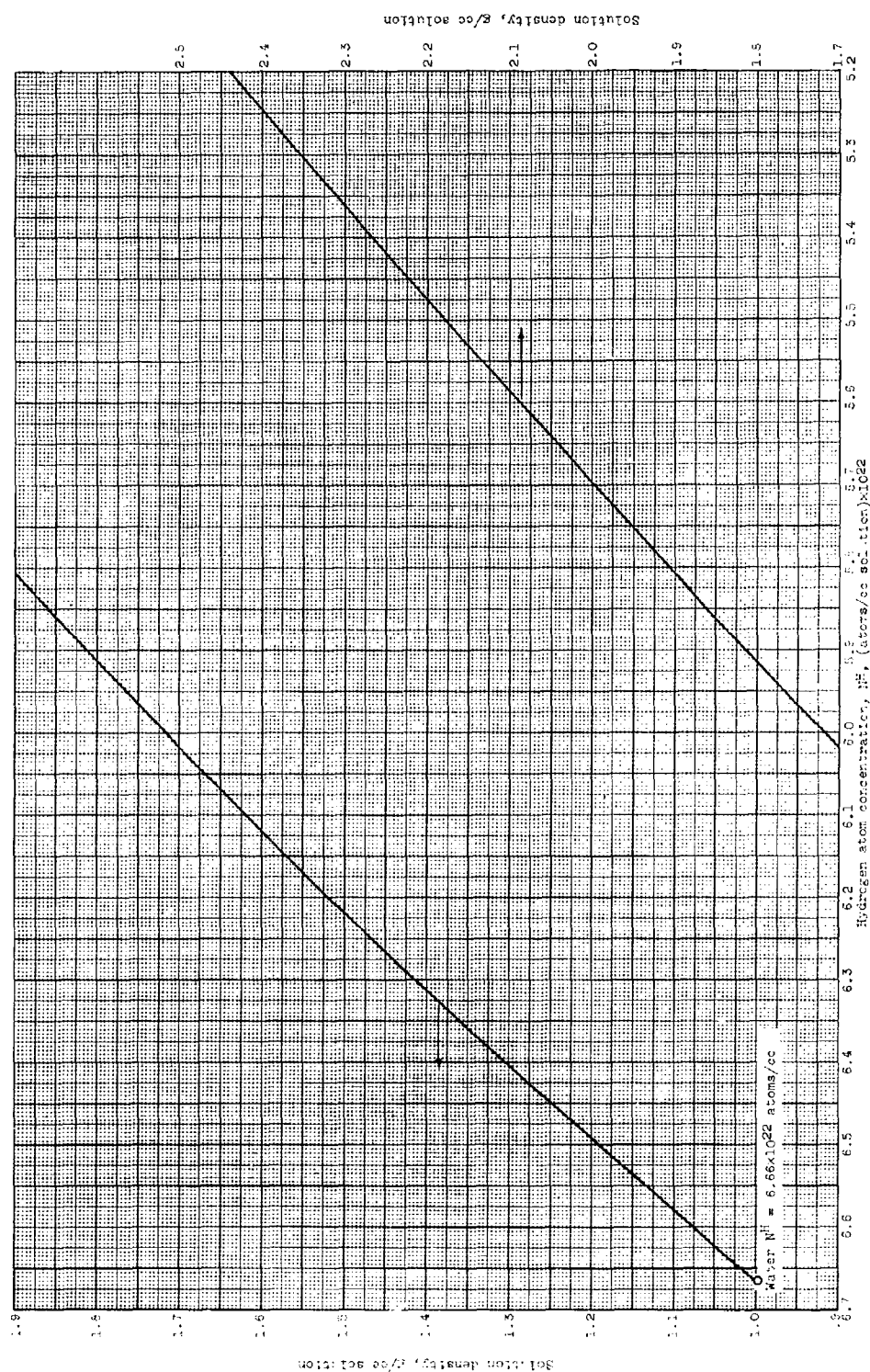
Figure 2. - Density of UO_2F_2-H_2O solutions at 25° C. Uranium enriched to 0.932 U-235; water density 0.9970 gram per cubic centimeter.
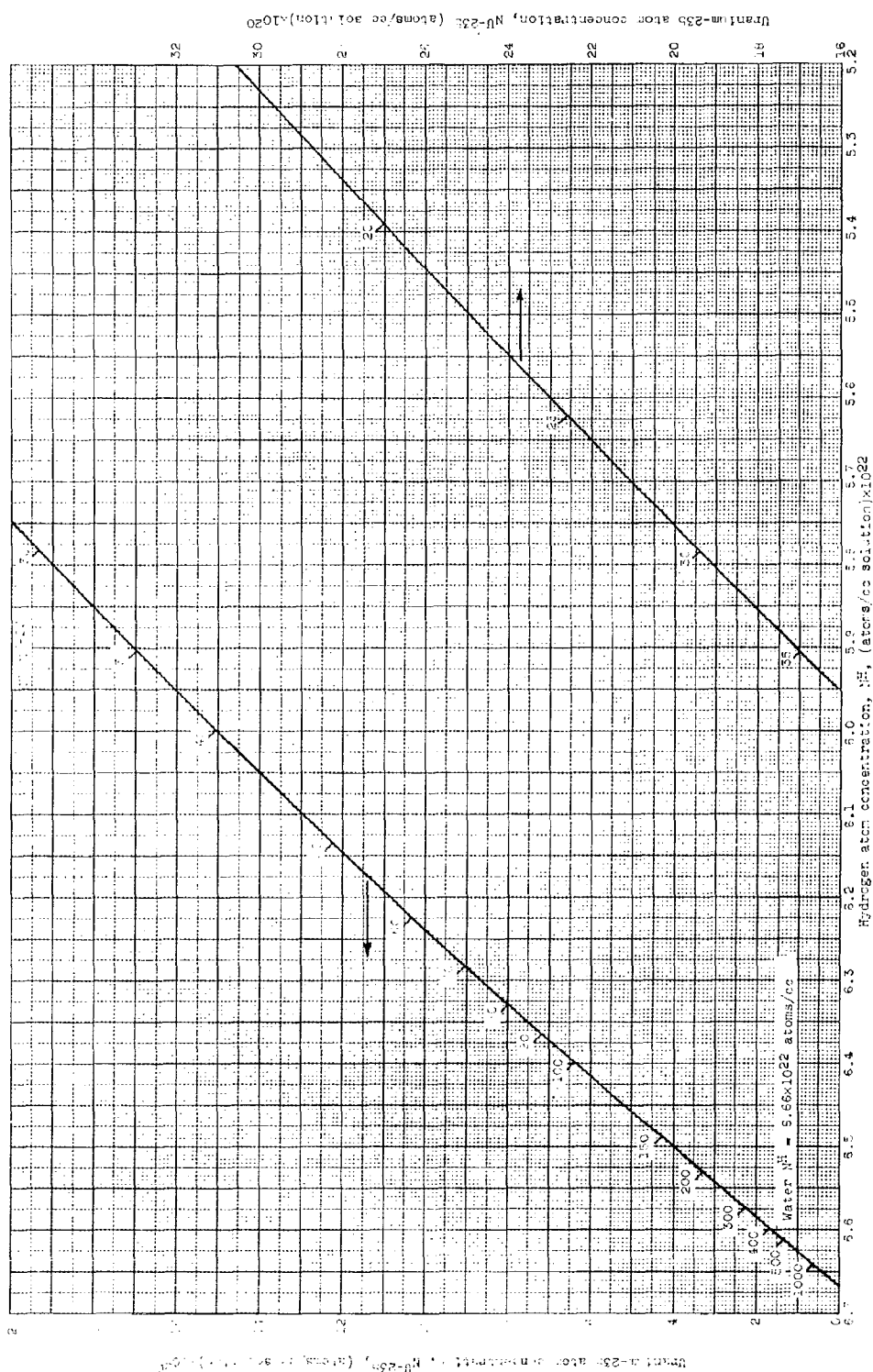
Figure 3. - Uranium-235 atom concentration in $UO_2F_2-H_2O$ solutions. Uranium enriched to 0.932 uranium-235; water at 25° C; density, 0.9970 gram per cubic centimeter.

E-69

E-690
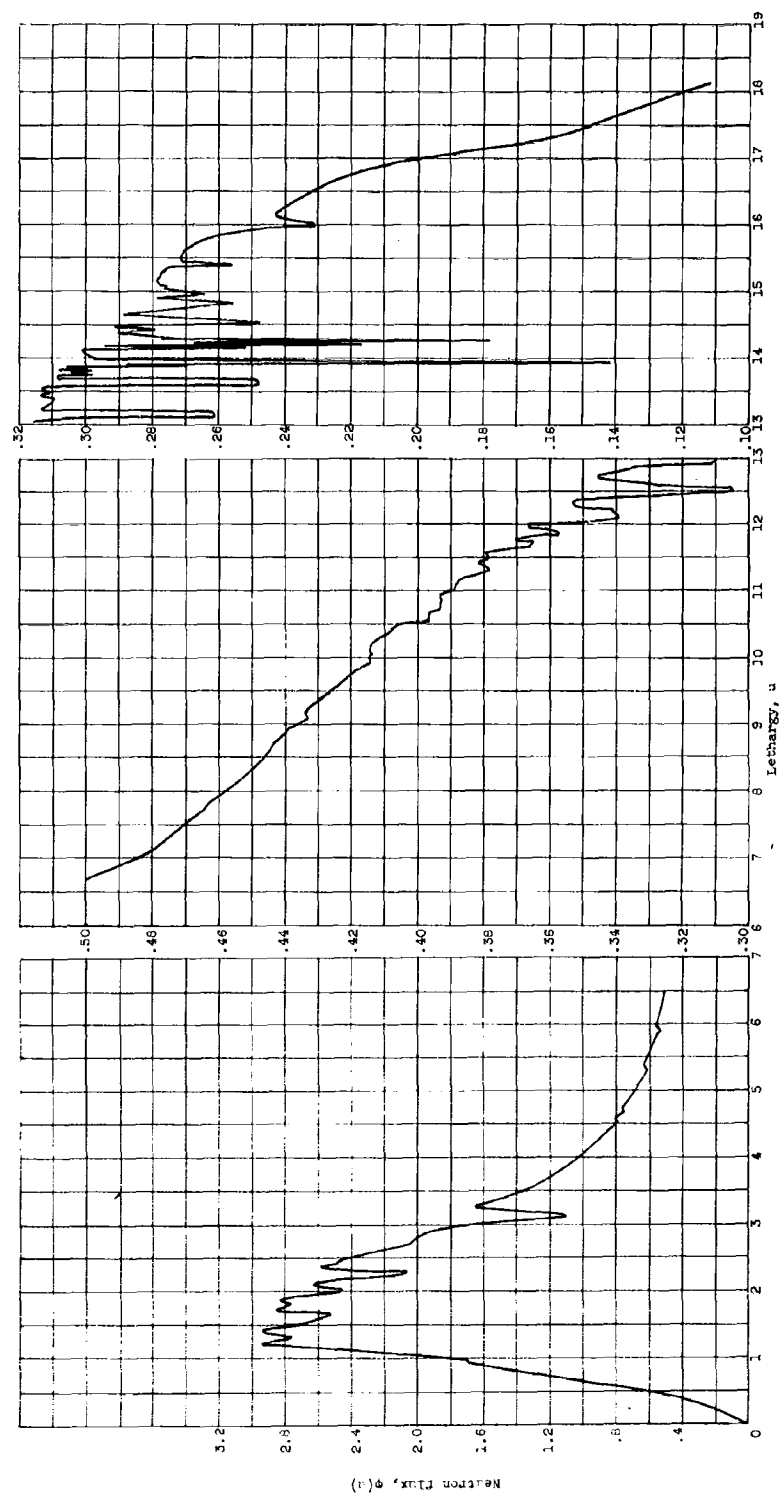
Figure 4. – Lethargy-dependent flux $\phi(u)$ plotted against lethargy u for a critical UO_2F_2 solution reactor of $N^H/N^{U-235} = 40$. Source normalization, 1 fission neutron. Thermal neutron flux $\phi_T = 0.4704$; $\int_0^{18.2} \phi(u)du = 12.582$.

36
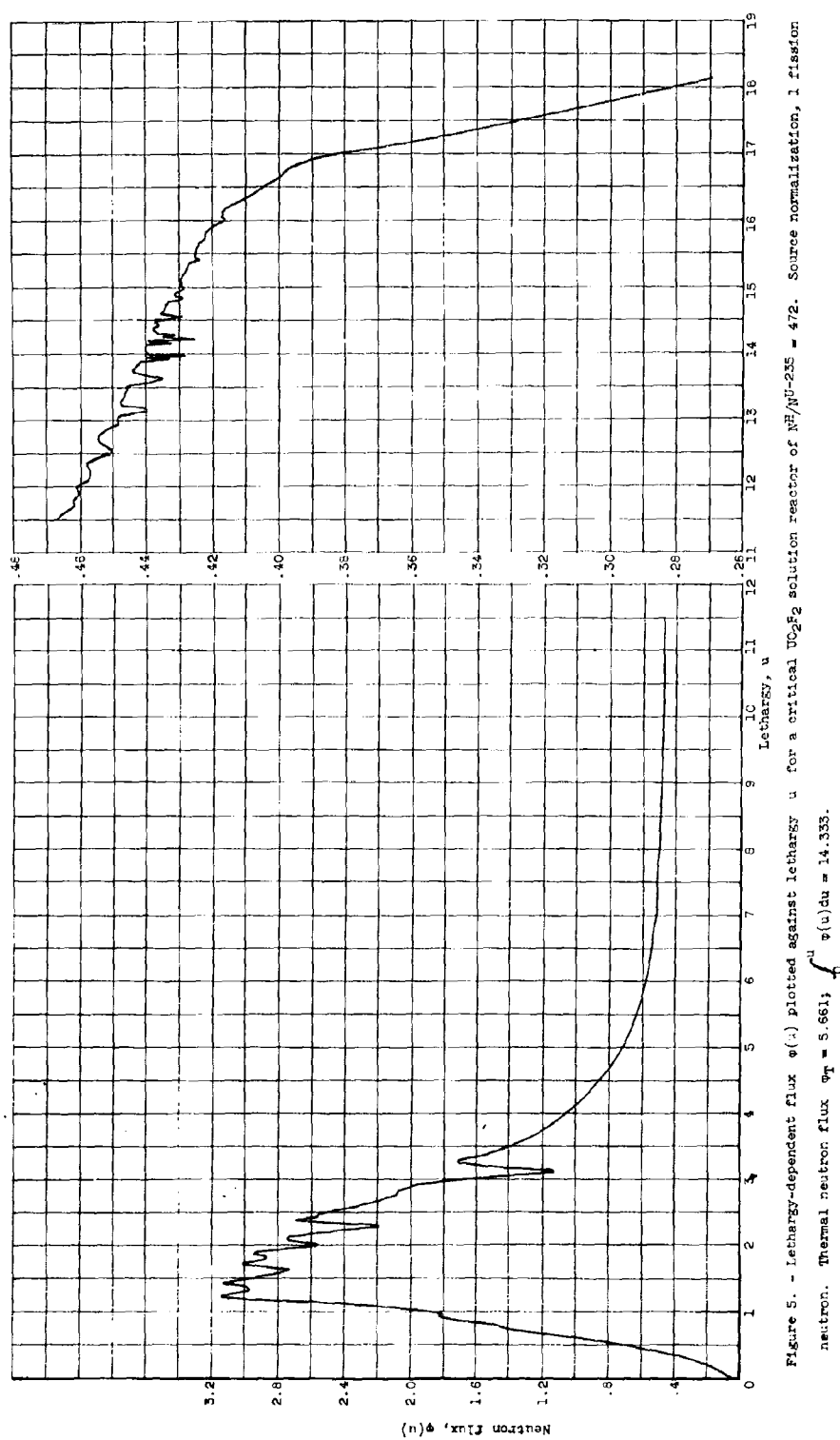
Figure 5. - Lethargy-dependent flux $\varphi(u)$ plotted against lethargy u for a critical UO_2F_2 solution reactor of $N^H/N^{U-235} = 472$. Source normalization, 1 fission neutron. Thermal neutron flux $\varphi_T = 5.661$; $\int_0^u \varphi(u) du = 14.333$.
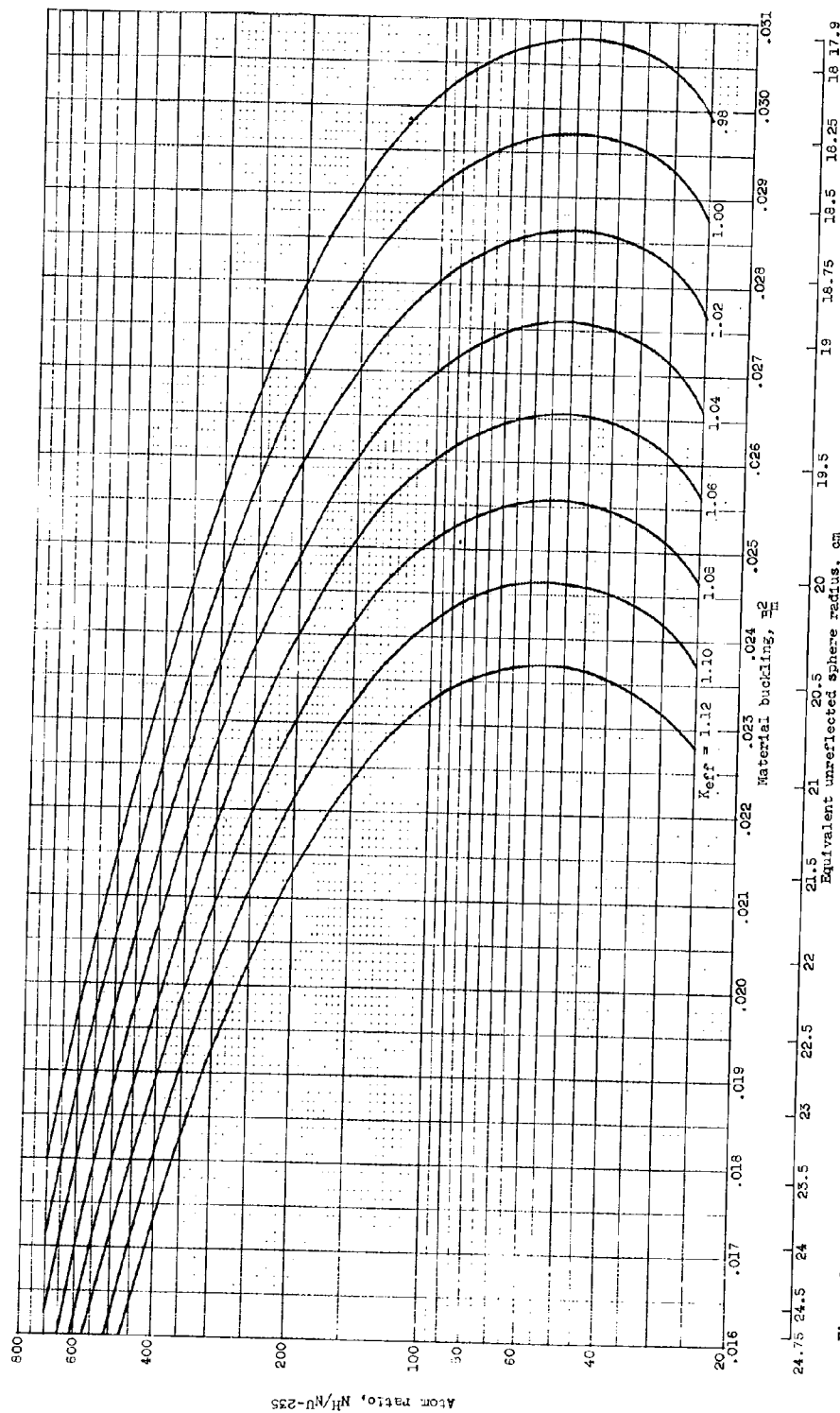
Figure 6. – Material buckling B_m^2 as a function of atom ratio N_H/NU-235 for various values of static criticality factor K_{eff} for unreflected UO_2F_2 solution reactors.
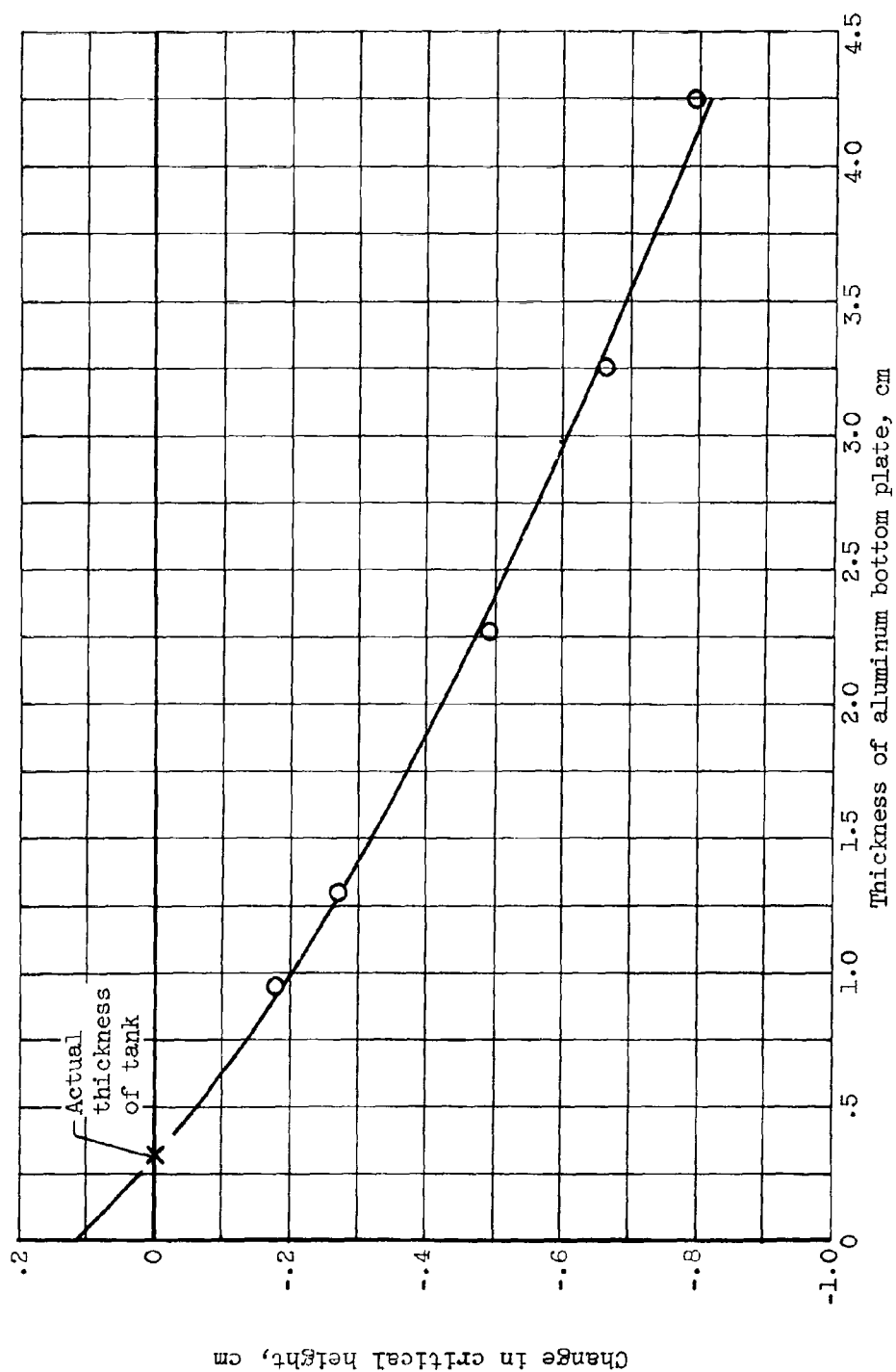
Figure 7. - Change in critical height of unreflected UO$_2$F$_2$ solution reactor contained in aluminum cylinder as a function of cylinder bottom plate thickness. NH/NU-235 = 475; diameter = 12 inches.
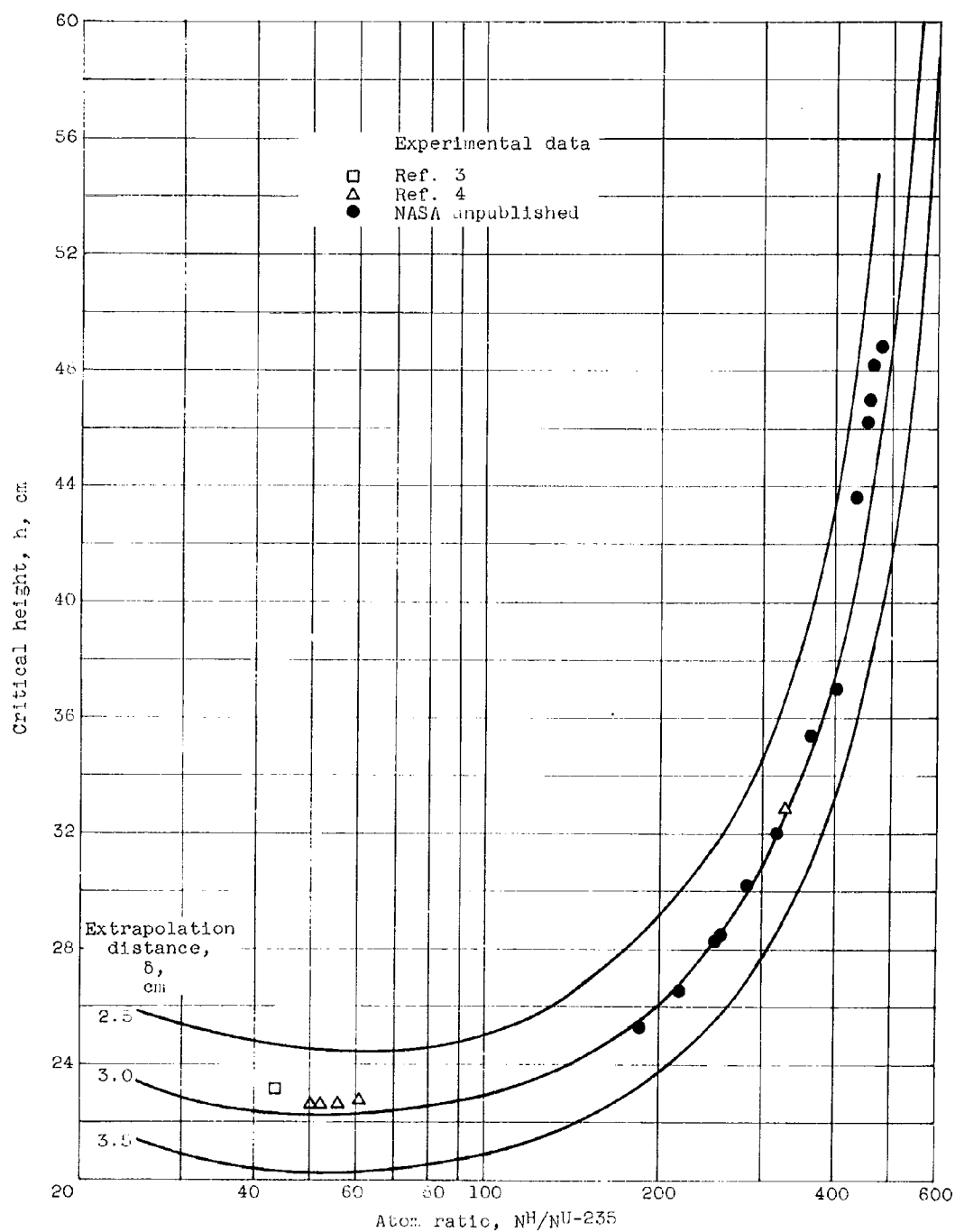
Figure 5. - Critical height for several values of extrapolation length plotted against atom ratio N^H/N^{U-235} for 12-inch-diameter unreflected UO_2F_2 solution reactors. Theoretical curves based on total buckling from figure 6.
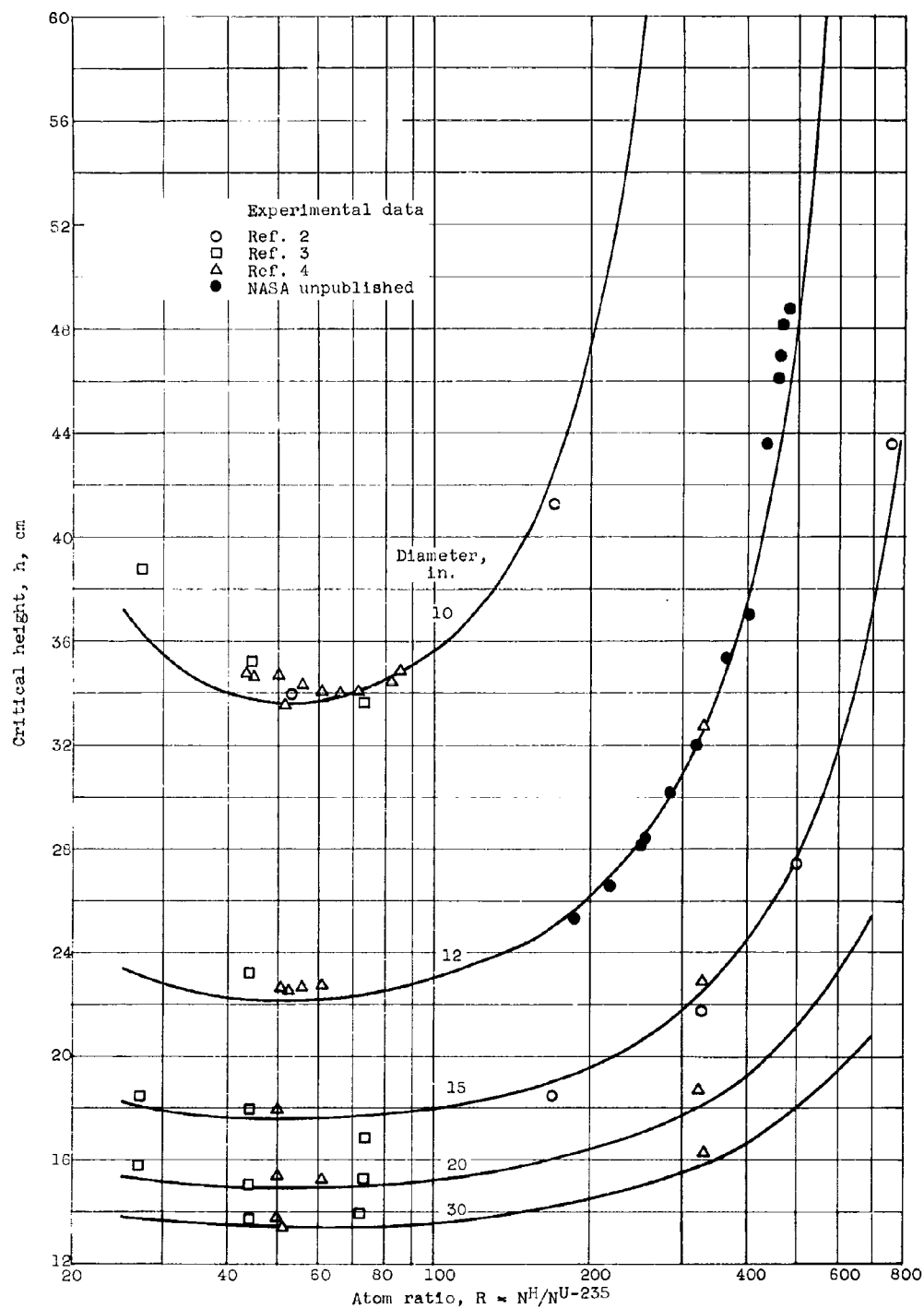
Figure 9. - Critical height plotted against atom ratio N^H/N^{U-235} for various diameters of unreflected UO_2F_2 solution reactors. (Theoretical curves based on total buckling from figure 6 and extrapolation distance $\delta = 3.0$ cm.)

E-690
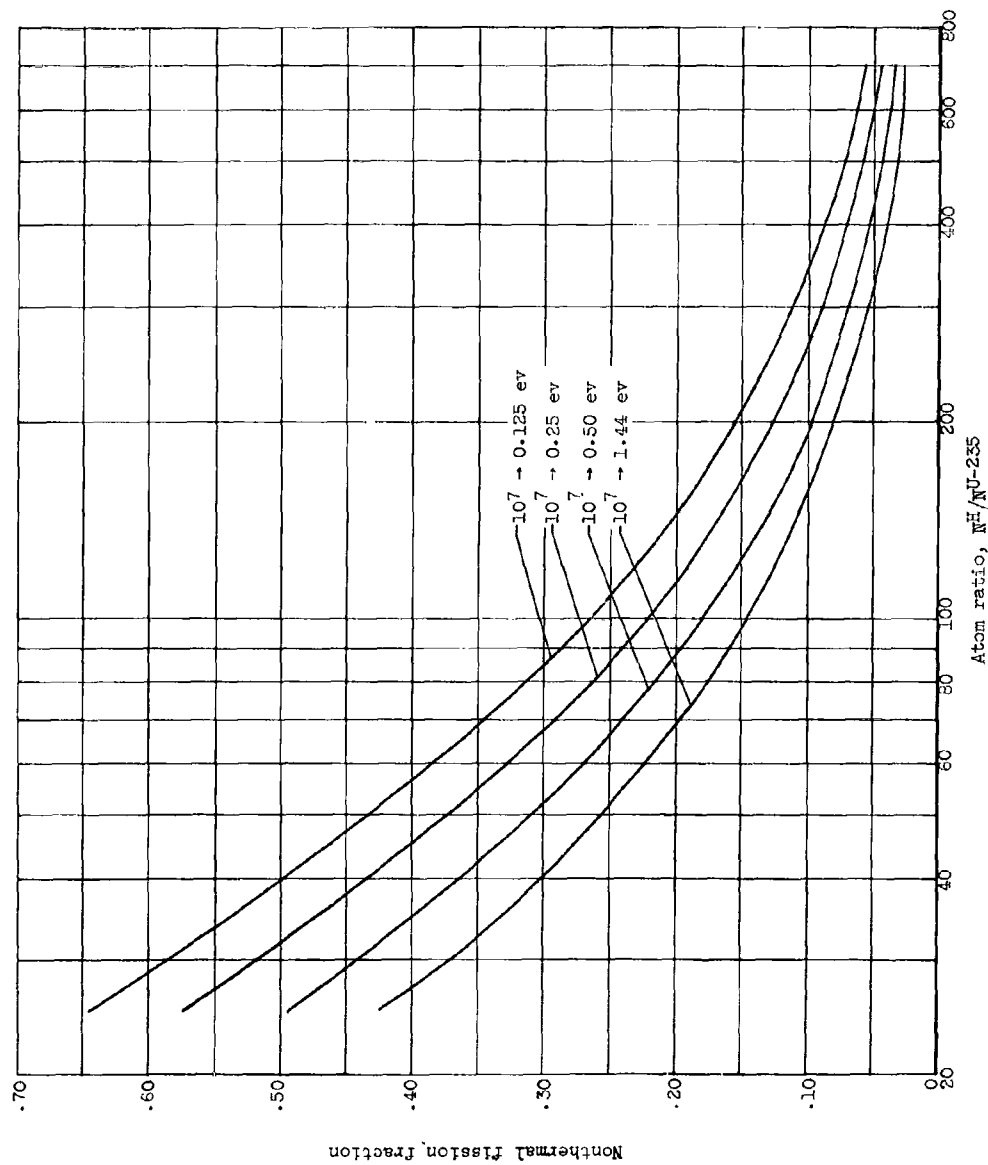
Figure 10. - Fraction of nonthermal fissions to total fissions plotted against atom ratio
N^H/N^{U-235} for several cutoff energies for UO_2F_2-H_2O solution reactors.
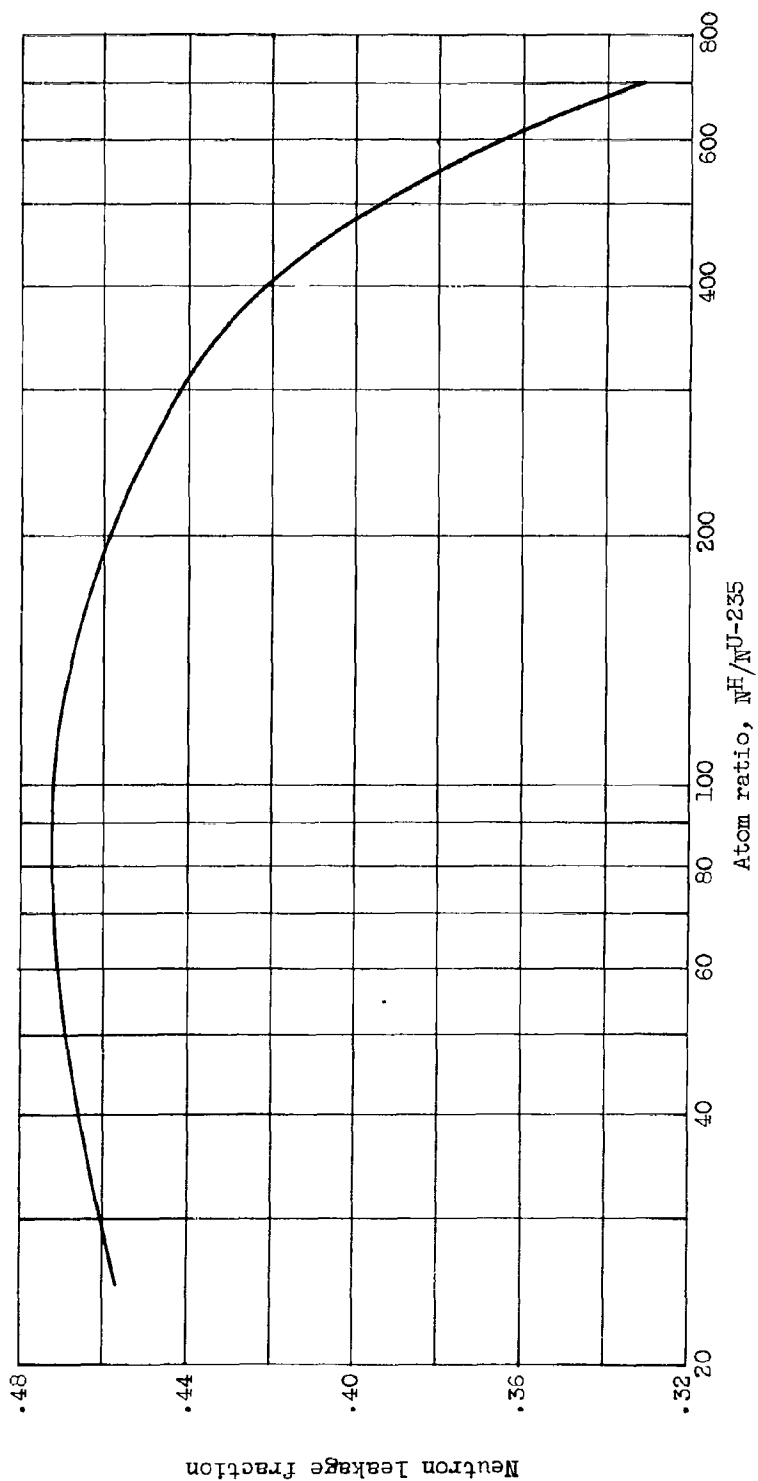
Figure 11. - Fraction of neutrons which escape from unreflected critical UO_2F_2 solution reactors as a function of atom ratio N^H/N^{U-235}.

Neutron leakage fraction

Atom ratio, N^H/N^{U-235}

E-690
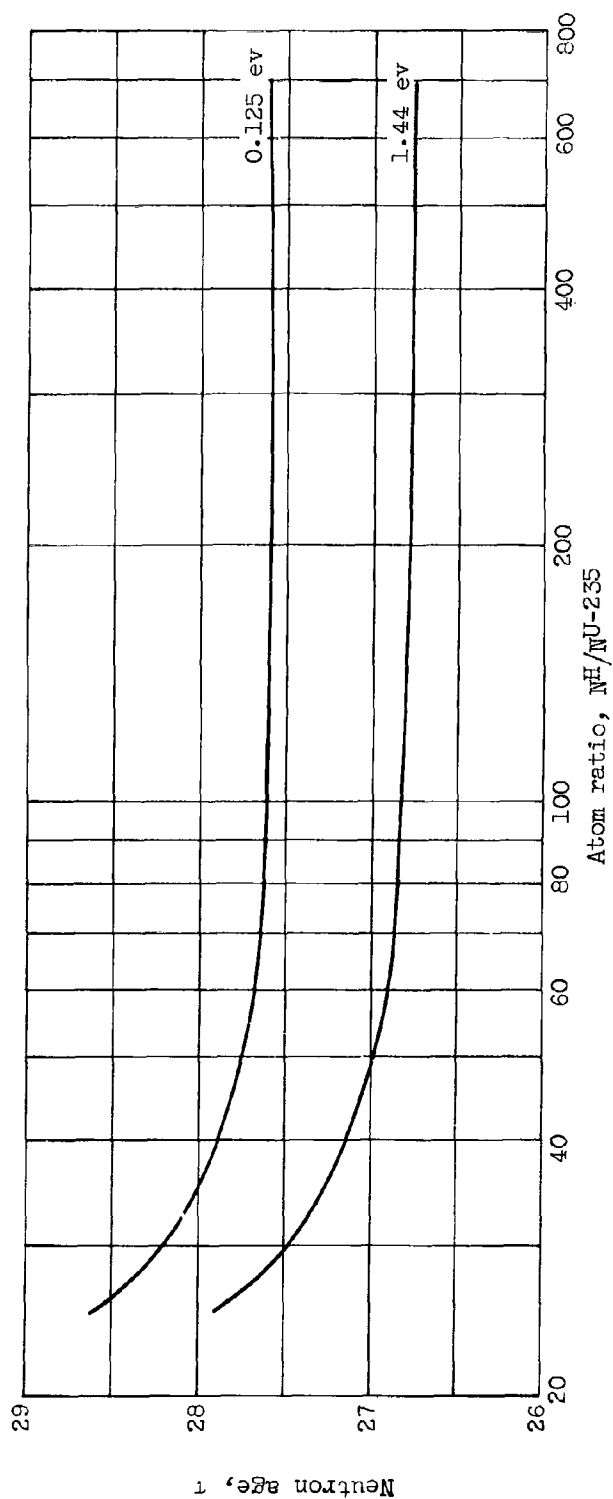
Figure 12. - Fission neutron age τ as a function of atom ratio N^H/N^{U-235} to indium resonance energy (1.44 ev) and to thermal cutoff energy (0.125 ev = 5 kT) for UO_2F_2-H_2O solution reactors.
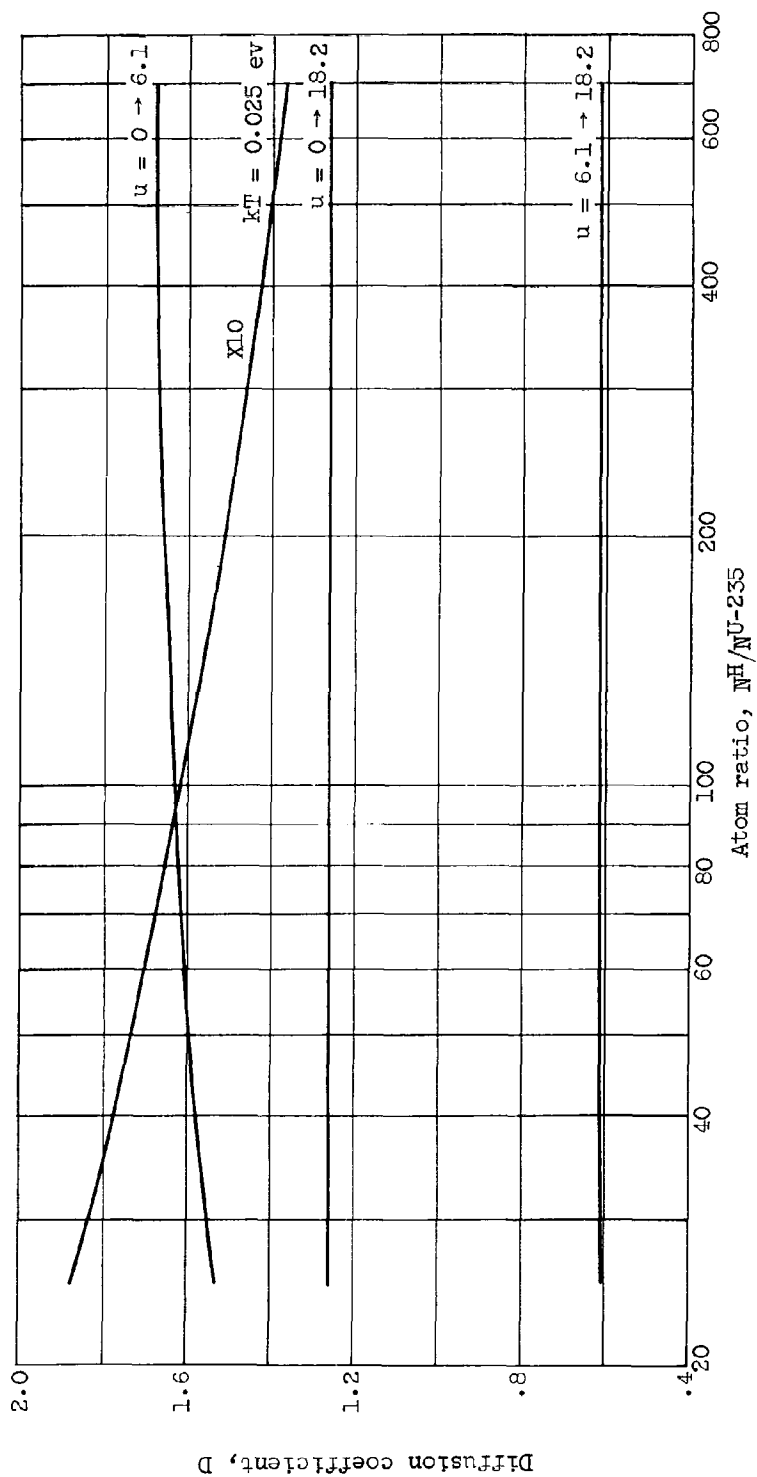
Figure 13. - Two- and three-group diffusion coefficients D plotted against atom ratio N^H/N^{U-235} for the UO_2F_2 solution reactors.
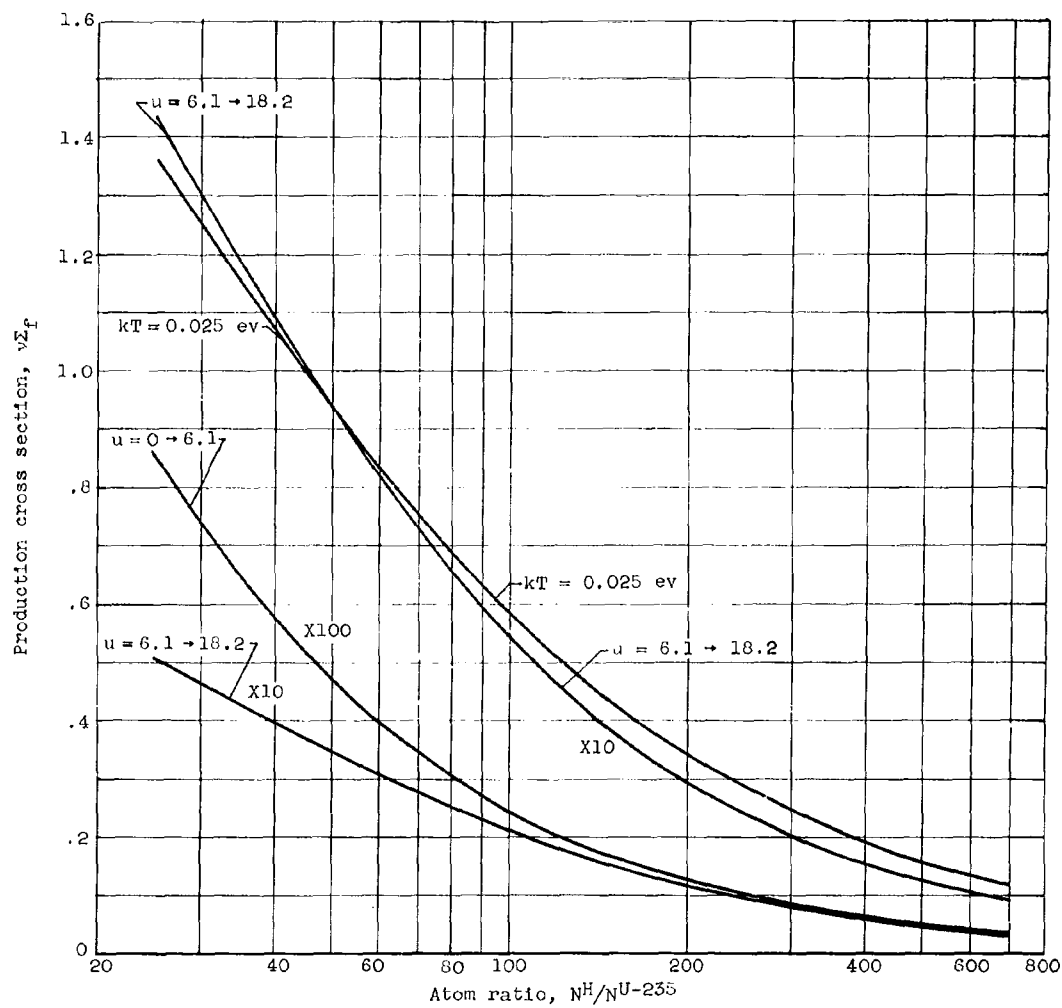
E-690
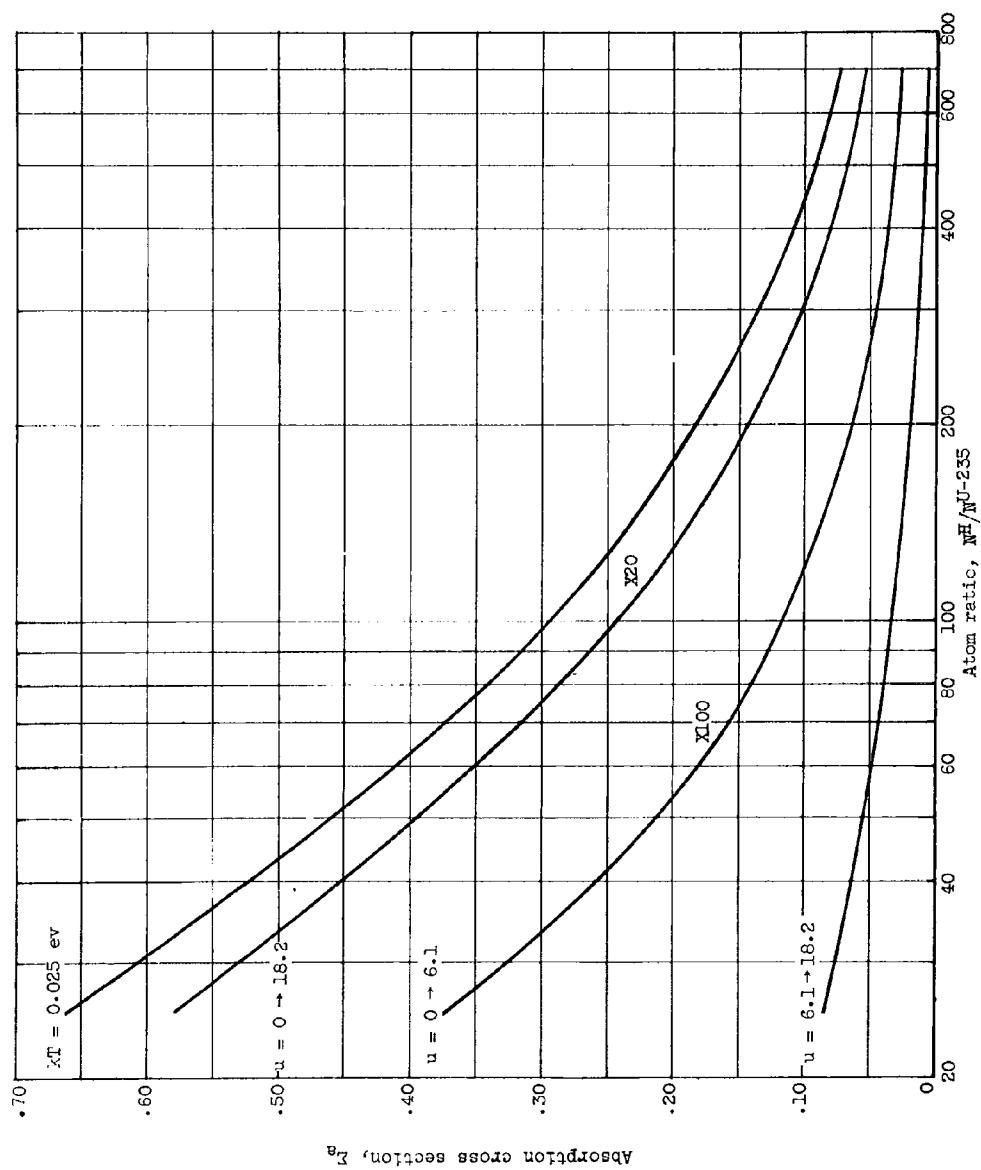
Figure 14. – Two and three-group absorption cross sections Σ_a plotted against atom ratio N^H/N^{U-235} for UO_2F_2 solution reactor.

Figure 15. - Two- and three-group production cross sections $\nu\Sigma_f$ plotted against atom ratio N^H/N^{U-235} for UO_2F_2 solution reactors
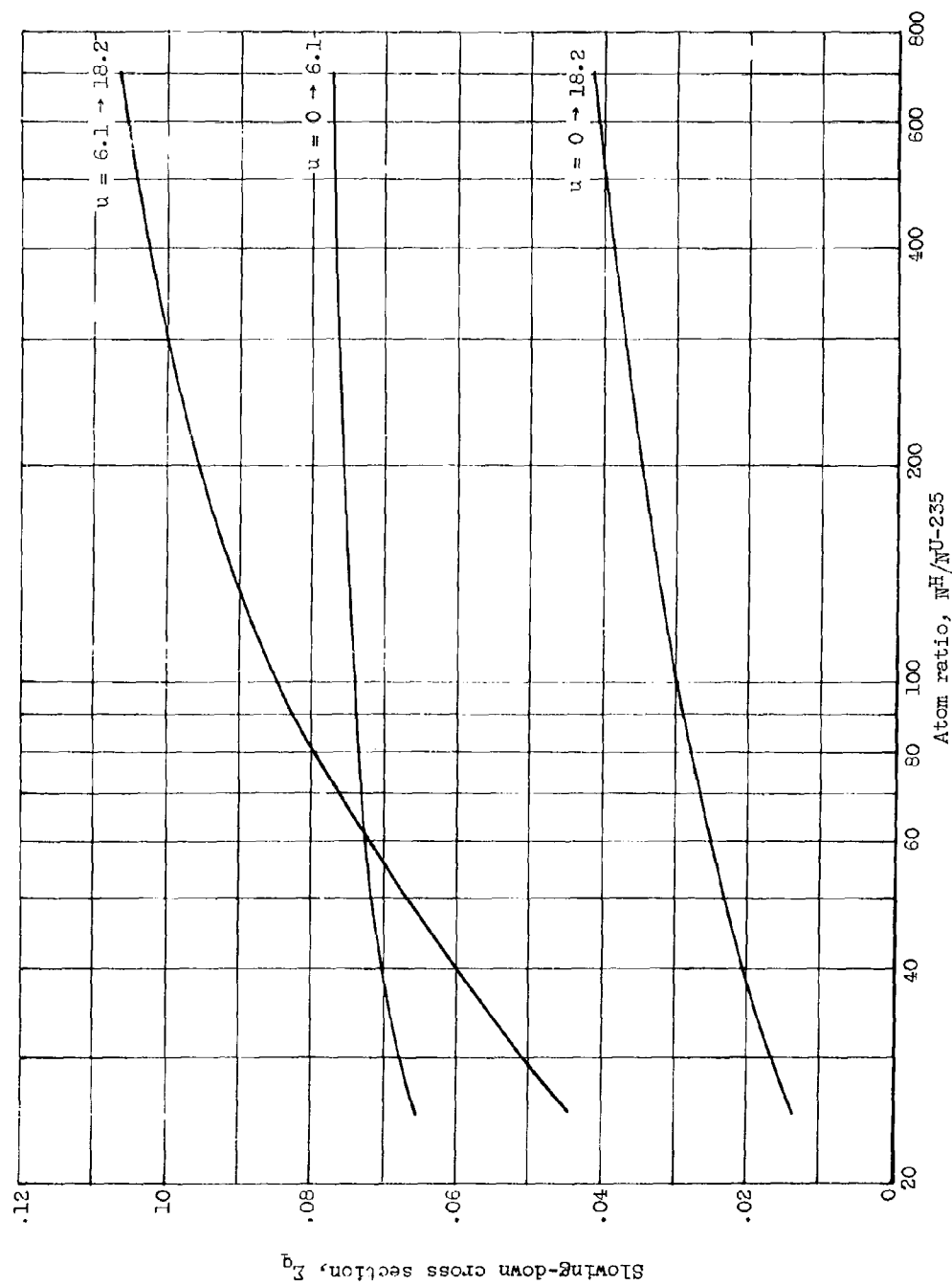
E-690

u = 6.1 → 18.2

u = 0 → 6.1

u = 0 → 18.2

.12

.10

.08

.06

.04

.02

0

20   40   60   80   100   200   400   600   800

Atom ratio, N^H/N^{U-235}

Slowing-down cross section, Σ_q

Figure 16. – Two- and three-group slowing-down cross sections Σ_q as a function of atom ratio N^H/N^{U-235} for UO_2F_2 solution reactor.
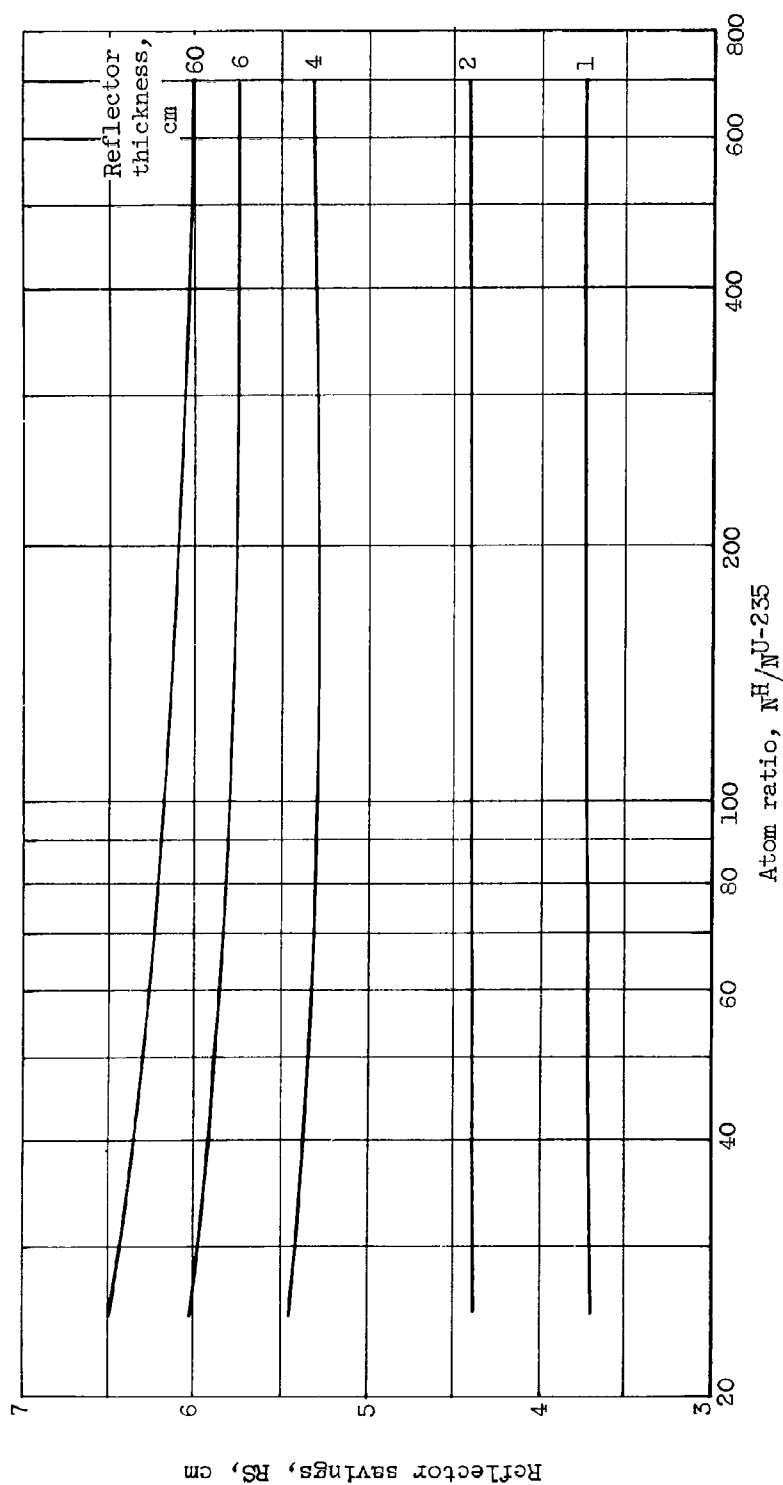
Figure 17. - Reflector savings calculated using a three-group spherical model for various thicknesses of water reflector as a function of atom ratio N^H/N^{U-235}.
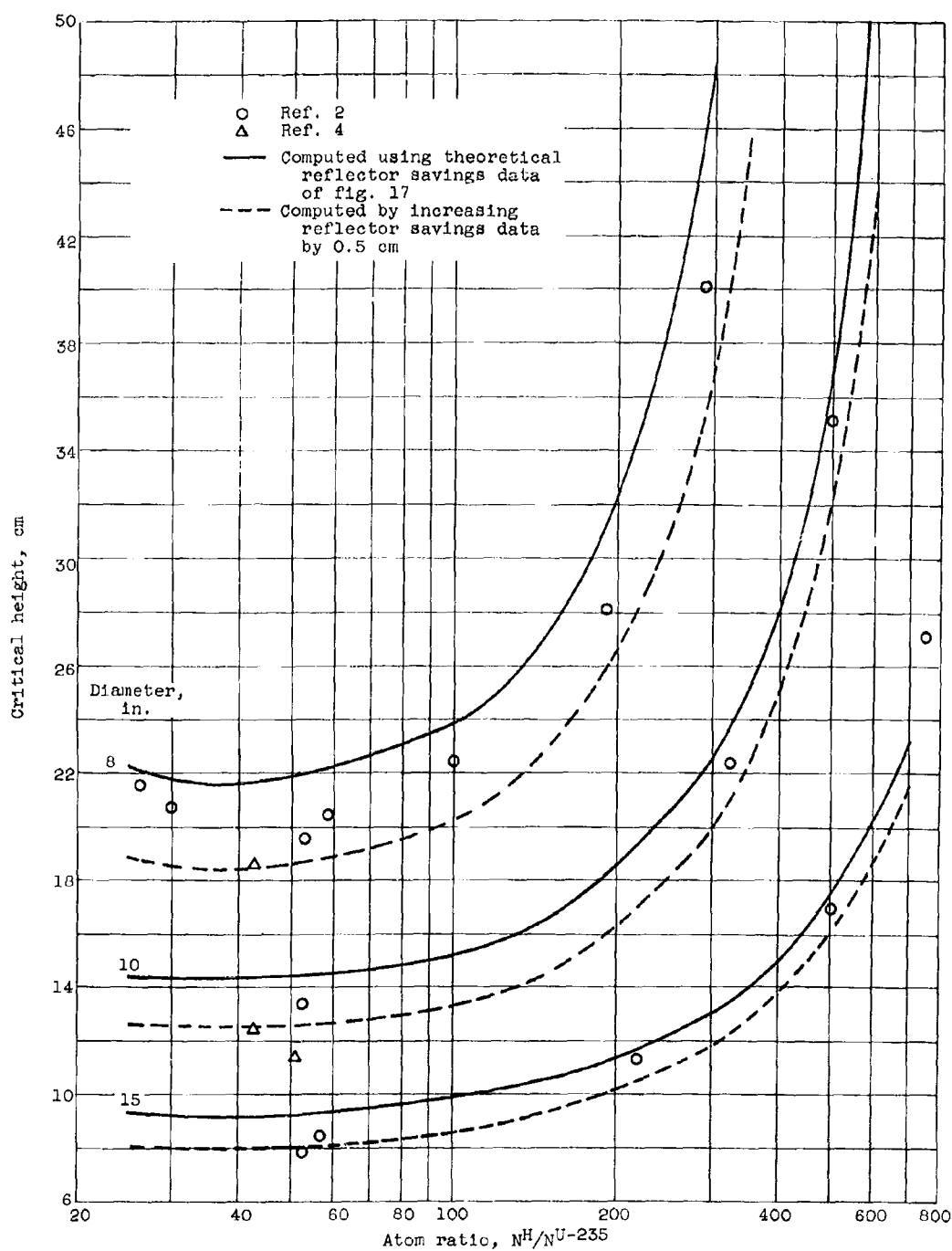
Figure 18. - Critical height plotted against atom ratio N^H/N^{U-235} for various diameters of cylindrical UO_2F_2 solution reactors having both end and side reflectors of water (infinite thickness). Theoretical curves obtained using calculated values of total buckling given in figure 6 and reflector savings given in figure 17.

NASA TN D-1102
National Aeronautics and Space Administration.
CONSISTENT P1 ANALYSIS OF AQUEOUS URANIUM-
235 CRITICAL ASSEMBLIES. Daniel Fieno.
November 1961. 49p. OTS price, $1.25.
(NASA TECHNICAL NOTE D-1102)

The lethargy-dependent consistent P1 equations
describing the neutron slowing-down process are
developed for use on the IBM 704 electronic computer.
Effects included are (1) linearly anisotropic center of
mass elastic scattering, (2) heavy element inelastic
scattering based on the evaporation model of the
nucleus, and (3) optional variation of the buckling with
lethargy. The microscopic cross-section data used
for this program are briefly discussed. The method
is applied to the calculation of the neutron age in
water, the Fourier transform of the slowing-down
kernel in water, and the critical dimensions of unre-
flected and fully water-reflected uranyl fluoride -
water solution critical assemblies.

Copies obtainable from NASA, Washington

NASA

I. Fieno, Daniel
II. NASA TN D-1102

(Initial NASA distribution:
31, Physics, nuclear and
particle; 42, Propulsion
systems, nuclear.)

NASA TN D-1102
National Aeronautics and Space Administration.
CONSISTENT P1 ANALYSIS OF AQUEOUS URANIUM-
235 CRITICAL ASSEMBLIES. Daniel Fieno.
November 1961. 49p. OTS price, $1.25.
(NASA TECHNICAL NOTE D-1102)

The lethargy-dependent consistent P1 equations
describing the neutron slowing-down process are
developed for use on the IBM 704 electronic computer.
Effects included are (1) linearly anisotropic center of
mass elastic scattering, (2) heavy element inelastic
scattering based on the evaporation model of the
nucleus, and (3) optional variation of the buckling with
lethargy. The microscopic cross-section data used
for this program are briefly discussed. The method
is applied to the calculation of the neutron age in
water, the Fourier transform of the slowing-down
kernel in water, and the critical dimensions of unre-
flected and fully water-reflected uranyl fluoride -
water solution critical assemblies.

Copies obtainable from NASA, Washington

NASA

I. Fieno, Daniel
II. NASA TN D-1102

(Initial NASA distribution:
31, Physics, nuclear and
particle; 42, Propulsion
systems, nuclear.)

NASA TN D-1102
National Aeronautics and Space Administration.
CONSISTENT P1 ANALYSIS OF AQUEOUS URANIUM-
235 CRITICAL ASSEMBLIES. Daniel Fieno.
November 1961. 49p. OTS price, $1.25.
(NASA TECHNICAL NOTE D-1102)

The lethargy-dependent consistent P1 equations
describing the neutron slowing-down process are
developed for use on the IBM 704 electronic computer.
Effects included are (1) linearly anisotropic center of
mass elastic scattering, (2) heavy element inelastic
scattering based on the evaporation model of the
nucleus, and (3) optional variation of the buckling with
lethargy. The microscopic cross-section data used
for this program are briefly discussed. The method
is applied to the calculation of the neutron age in
water, the Fourier transform of the slowing-down
kernel in water, and the critical dimensions of unre-
flected and fully water-reflected uranyl fluoride -
water solution critical assemblies.

Copies obtainable from NASA, Washington

NASA

I. Fieno, Daniel
II. NASA TN D-1102

(Initial NASA distribution:
31, Physics, nuclear and
particle; 42, Propulsion
systems, nuclear.)

NASA TN D-1102
National Aeronautics and Space Administration.
CONSISTENT P1 ANALYSIS OF AQUEOUS URANIUM-
235 CRITICAL ASSEMBLIES. Daniel Fieno.
November 1961. 49p. OTS price, $1.25.
(NASA TECHNICAL NOTE D-1102)

The lethargy-dependent consistent P1 equations
describing the neutron slowing-down process are
developed for use on the IBM 704 electronic computer.
Effects included are (1) linearly anisotropic center of
mass elastic scattering, (2) heavy element inelastic
scattering based on the evaporation model of the
nucleus, and (3) optional variation of the buckling with
lethargy. The microscopic cross-section data used
for this program are briefly discussed. The method
is applied to the calculation of the neutron age in
water, the Fourier transform of the slowing-down
kernel in water, and the critical dimensions of unre-
flected and fully water-reflected uranyl fluoride -
water solution critical assemblies.

Copies obtainable from NASA, Washington

NASA

I. Fieno, Daniel
II. NASA TN D-1102

(Initial NASA distribution:
31, Physics, nuclear and
particle; 42, Propulsion
systems, nuclear.)